



Article

Liraglutide Protects Against Brain Amyloid- β_{1-42} Accumulation in Female Mice with Early Alzheimer's Disease-Like Pathology by Partially Rescuing Oxidative/Nitrosative Stress and Inflammation

Ana I. Duarte ^{1,2,3,*} , Emanuel Candeias ^{1,2,3,†}, Inês N. Alves ^{1,3,4} , Débora Mena ^{1,3,4} , Daniela F. Silva ¹ , Nuno J. Machado ¹ , Elisa J. Campos ^{3,5}, Maria S. Santos ^{1,6}, Catarina R. Oliveira ^{1,3,7} and Paula I. Moreira ^{1,3,8,*}

¹ CNC—Center for Neuroscience and Cell Biology, Rua Larga, Faculty of Medicine (Pólo 1, 1st Floor), University of Coimbra, 3004-504 Coimbra, Portugal; eu.emago@hotmail.com (E.C.); minalves09@gmail.com (I.N.A.); deboramena1996@gmail.com (D.M.); dani_malyk@hotmail.com (D.F.S.); nihonmeru@yahoo.co.uk (N.J.M.); mssantos@ci.uc.pt (M.S.S.); Catarina.n.oliveira@gmail.com (C.R.O.)

² Institute for Interdisciplinary Research (IIIUC), University of Coimbra, Casa Costa Alemão-Pólo II, Rua D. Francisco de Lemos, 3030-789 Coimbra, Portugal

³ Center for Innovative Biomedicine and Biotechnology (CIBB), Rua Larga, Faculty of Medicine (Pólo 1, 1st Floor), University of Coimbra, 3004-504 Coimbra, Portugal; elisajcampos@uc.pt

⁴ Faculty of Medicine, University of Coimbra, 3004-504 Coimbra, Portugal

⁵ Coimbra Institute for Clinical and Biomedical Research (iCBR), Faculty of Medicine, University of Coimbra, 3000-548 Coimbra, Portugal

⁶ Life Sciences Department, University of Coimbra, Largo Marquês de Pombal, 3004-517 Coimbra, Portugal

⁷ Institute of Biochemistry, Faculty of Medicine, University of Coimbra, 3000-548 Coimbra, Portugal

⁸ Institute of Physiology, Faculty of Medicine, University of Coimbra, 3000-548 Coimbra, Portugal

* Correspondence: ana.duarte@cnc.uc.pt (A.I.D.); pimoreira@fmed.uc.pt (P.I.M.); Tel.: +351-239-820190 (A.I.D.); +351-239-820190 (P.I.M.); Fax: +351-239-822776 (A.I.D.); +351-239-822776 (P.I.M.)

† These authors contributed equally to this work.

Received: 9 December 2019; Accepted: 28 February 2020; Published: 4 March 2020



Abstract: Alzheimer's disease (AD) is the most common form of dementia worldwide, being characterized by the deposition of senile plaques, neurofibrillary tangles (enriched in the amyloid beta (A β) peptide and hyperphosphorylated tau (p-tau), respectively) and memory loss. Aging, type 2 diabetes (T2D) and female sex (especially after menopause) are risk factors for AD, but their crosslinking mechanisms remain unclear. Most clinical trials targeting AD neuropathology failed and it remains incurable. However, evidence suggests that effective anti-T2D drugs, such as the GLP-1 mimetic and neuroprotector liraglutide, can be also efficient against AD. Thus, we aimed to study the benefits of a peripheral liraglutide treatment in AD female mice. We used blood and brain cortical lysates from 10-month-old 3xTg-AD female mice, treated for 28 days with liraglutide (0.2 mg/kg, once/day) to evaluate parameters affected in AD (e.g., A β and p-tau, motor and cognitive function, glucose metabolism, inflammation and oxidative/nitrosative stress). Despite the limited signs of cognitive changes in mature female mice, liraglutide only reduced their cortical A β_{1-42} levels. Liraglutide partially attenuated brain estradiol and GLP-1 and activated PKA levels, oxidative/nitrosative stress and inflammation in these AD female mice. Our results support the earlier use of liraglutide as a potential preventive/therapeutic agent against the accumulation of the first neuropathological features of AD in females.

Keywords: Alzheimer's disease; brain protection; female sex; GLP-1 mimetics; liraglutide

1. Introduction

Alzheimer's disease (AD) is the most common neurodegenerative disorder, neuropathologically characterized by the accumulation of senile plaques and neurofibrillary tangles (mainly composed of amyloid beta ($A\beta$) peptide and hyperphosphorylated tau protein (p-tau), respectively) [1,2]. Its most common clinical symptom is the progressive loss of memory [3].

Two-thirds of AD patients are women, >60% of them at menopause [4]. This renders female sex the major risk factor for sporadic AD after aging [5], with its pathophysiological action starting years to decades before the onset of clinical symptoms, most likely at midlife—the so-called prodromal or preclinical phase [6]. Indeed, studies showed that perimenopausal and menopausal women have a higher metabolic decline and $A\beta$ levels, alongside a greater atrophy of grey and white matter relative to premenopausal women and age-matched men [7,8]. Although the involved mechanisms remain debatable, the hormonal fluctuations affecting women from midlife until advanced ages may render them more vulnerable to brain changes and AD [7–10]. In this respect, early changes in serum estrogen levels were correlated with cognitive impairment years later in aged women [11], and with cortical and hippocampal senile plaque formation and memory deficits in AD female mice [12–17]. This, together with the estimates that 2/3 of AD caregivers are women render them at the epicenter of this epidemic [7,8].

AD is closely connected with diabetes (particularly type 2 diabetes; T2D) and obesity—both considered risk factors for AD. Although evidence suggests that AD patients may be more prone to develop co-morbid diabetes or obesity, this remains debatable [18–20]. Nevertheless, the features shared by these pathologies (e.g., impaired insulin signaling, and brain glucose transport and metabolism, mitochondrial anomalies, redox imbalance, inflammation and cognitive deficits [20,21]), alongside the failure of most AD clinical trials, led to the hypothesis that antidiabetic drugs may have a therapeutic potential against AD. Among them, glucagon-like peptide-1 (GLP-1) analogs are highly promising, with a minimal hypoglycemic risk. Similar to endogenous GLP-1, they tightly regulate postprandial blood glucose-dependent insulin secretion, with a subsequent fall in glycemia [22]. GLP-1 is also ubiquitously expressed in the central nervous system (CNS), particularly in the hypothalamus, cortex, hippocampus, striatum, substantia nigra, brainstem and subventricular zone, where it may play a pivotal role [23]. Indeed, modulation of GLP-1 receptor protected against neurodegenerative events, neuronal death and cognitive decline [24,25]. Additionally, the GLP-1 mimetic liraglutide mitigated synaptic loss and neuropathology, and improved learning and memory in male AD mice [26,27]. Liraglutide also rescued hyperhomocysteinemia-induced AD pathology and memory deficits in rats [28]. Although the involved mechanisms remain unclear, liraglutide may recover brain insulin receptors (IR) and synapses after $A\beta$ oligomer injection, ultimately improving memory function in mice and in non-human primates [29]. Liraglutide also hampered $A\beta$ plaque formation [30], astrocyte- and microglia-mediated inflammation [31] and promoted neurogenesis and neuronal proliferation [32].

The lack of efficient AD-modifying therapies may result from studies performed in already symptomatic cohorts (with synaptic and neuronal deficits) and/or from the underestimation of sex differences in AD pathophysiology [33]. Moreover, most studies were performed in the hippocampus, despite the AD effects on wide areas of cerebral cortex [34,35] (including the frontal cortex) that underlie cognitive function and metabolic regulation [36]. Thus, there is an urgent need to uncover the role of female sex on brain cortical AD pathophysiology and progression, and to establish novel therapeutic strategies against the disease. These, by starting during the prodromal phase of AD, may efficiently prevent or delay its onset, or blunt its progression [33]. In this perspective, we aimed to evaluate the therapeutic benefits of a chronic (28-day) liraglutide treatment in mature female mice with AD-like pathology. Thus, we analyzed several brain parameters traditionally affected by AD, namely glucose metabolism, mitochondrial function/dynamics, inflammation, oxidative stress, neuropathological features and motor and cognitive behavior.

As far as we know, only one study evaluated the effects of an 8-week liraglutide treatment in the 3xTg-AD mice, but in middle-aged (7–9 month-old) males [26]. This and our previous study in

11-month-old 3xTg-AD male mice [37] led us to use brain cortices from mature (10-month-old) 3xTg-AD female mice displaying AD-like pathology, treated with liraglutide for a shorter time (4 weeks). Our results suggest that, despite the limited signs of cognitive impairment in these mature female mice, liraglutide treatment only mitigated the increased accumulation of brain cortical $A\beta_{1-42}$. The drug also partially normalized their brain estradiol, GLP-1 content and PKA, partially reducing their plasma and brain inflammatory and oxidative stress markers, possibly due to the stimulation of glucose 6-phosphate dehydrogenase (G6PDH) (and its downstream antioxidant properties) and mitochondrial dynamics. As far as we know, this study constitutes a first approach to the use of GLP-1 mimetics (namely liraglutide) to mitigate some of the earlier AD-like pathological features in females. Further studies are needed to reinforce the need for a more tailored, sex/gender-based medicine.

2. Results

2.1. Effect of Liraglutide Treatment on Brain and Peripheral Features in Female Mice

The key neuropathological hallmarks of AD are the deposition of $A\beta$ and hyperphosphorylated tau that occur early in disease pathology in brain areas such as the hippocampus and cortex, long before its clinical diagnosis that relies mostly on memory loss and, to a lower extent, in a few biomarkers [18,38]. However, the precise crosslinking mechanisms that occur across this timeframe remain debatable.

Similar to our previous study in 11-month-old 3xTg-AD male mice [37], here we observed a significant increase in brain $A\beta_{1-42}$, $A\beta_{1-40}$ and p-tau(Ser396) levels in 3xTg-AD female mice compared to WT ones. Liraglutide treatment only reduced brain $A\beta_{1-42}$ levels (for $A\beta_{1-42}$: $F(2,14) = 15.206$; $p < 0.0001$; for $A\beta_{1-40}$: $F(2,14) = 4.597$; $p = 0.029$; for p-tau(Ser396): $F(2,11) = 10.178$; $p = 0.003$; Figure 1A–C). Despite this and our previous observations in mature 3xTg-AD male mice [37], our mature 3xTg-AD female mice only showed partial deficits in motor and cognitive performance compared to WT ones (Figure 2), as given by the slightly lower distance travelled in total ($F(2,18) = 0.609$; $p = 0.554$) and in the center of the open field arena ($F(2,17) = 2.141$; $p = 0.148$), and also by the time spent in its center ($Z = -0.387$, $p = 0.755$ for 3xTg-AD vs. WT mice; $Z = -0.579$, $p = 0.613$ for 3xTg-AD + Lira vs. WT mice; $Z = -0.429$, $p = 0.731$ for 3xTg-AD + Lira vs. 3xTg-AD mice), suggesting a thigmotaxic behavior that may be due to increased anxiety/fearfulness (Figure 2A–C). These were mirrored by their lower number of entries into the novel arm of the Y-maze ($F(2,20) = 8.454$; $p = 0.002$), despite no significant changes in the time spent in its start arm: $F(2,21) = 0.259$; $p = 0.774$) (Figure 2D,E), and the slightly reduced number of crossings of the Morris water maze ($Z = -1.787$, $p = 0.081$ for 3xTg-AD vs. WT mice; $Z = -0.059$, $p = 0.955$ for 3xTg-AD + Lira vs. WT mice; $Z = -1.619$, $p = 0.138$ for 3xTg-AD + Lira vs. 3xTg-AD mice; for escape latency: $Z = -0.698$, $p = 0.536$ for 3xTg-AD vs. WT mice; $Z = -0.901$, $p = 0.408$ for 3xTg-AD + Lira vs. WT mice; $Z = -0.457$, $p = 0.710$ for 3xTg-AD + Lira vs. 3xTg-AD mice) (Figure 2F–H), suggesting that the impairment in short-term spatial memory was not accompanied by significant changes in long-term spatial memory. Liraglutide administration only exerted limited benefits in these motor and cognitive deficits in mature 3xTg-AD female mice.

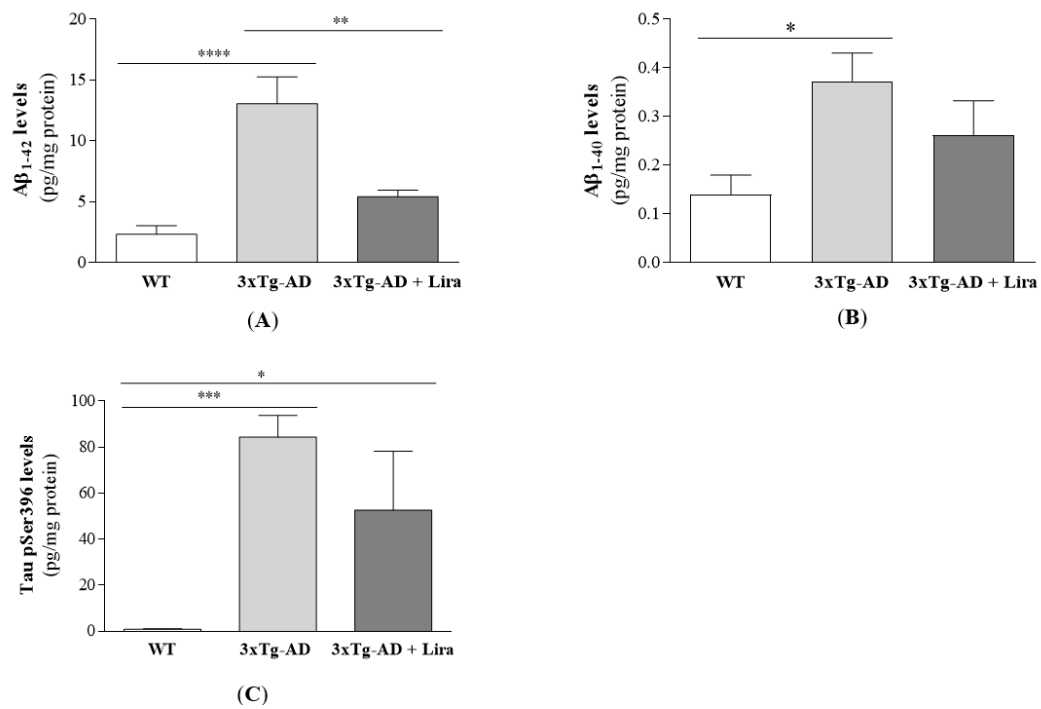


Figure 1. Effect of liraglutide on brain cortical AD-like hallmarks in 3xTg-AD female mice. Brain cortical Aβ₁₋₄₂ (A), Aβ₁₋₄₀ (B) and Tau pSer396 levels (C) were determined. Data are the mean ± SE from 4–6 mice/group. Statistical significance: * $p < 0.05$, ** $p < 0.01$, *** $p < 0.001$ or **** $p < 0.0001$, by the one-way ANOVA with the Bonferroni and Fisher LSD post-hoc tests for multiple comparisons.

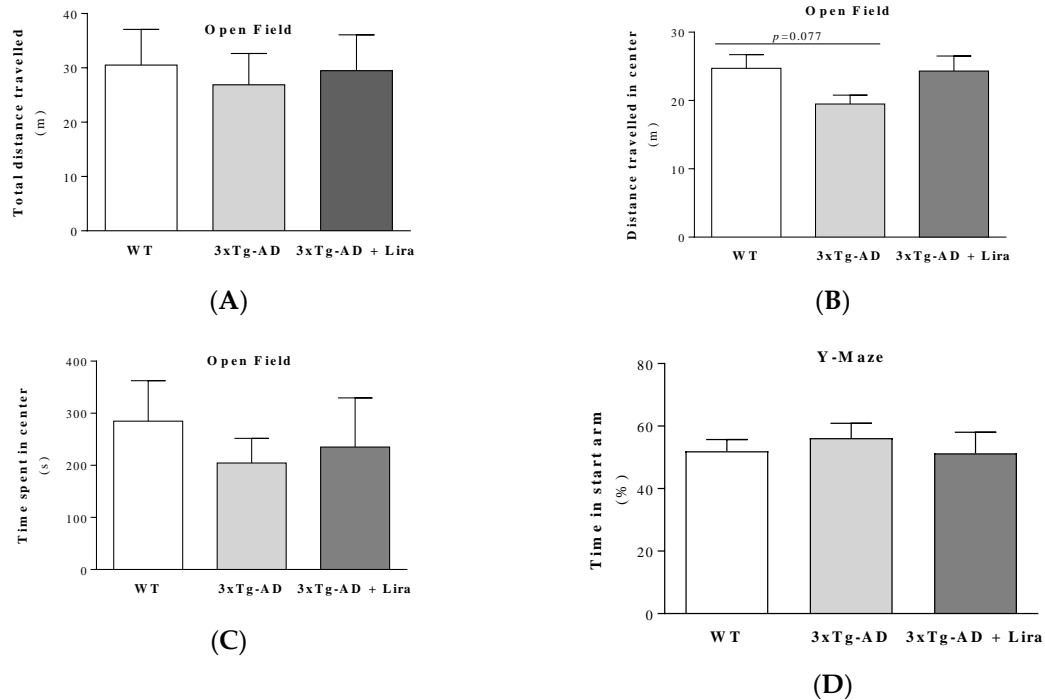


Figure 2. Cont.

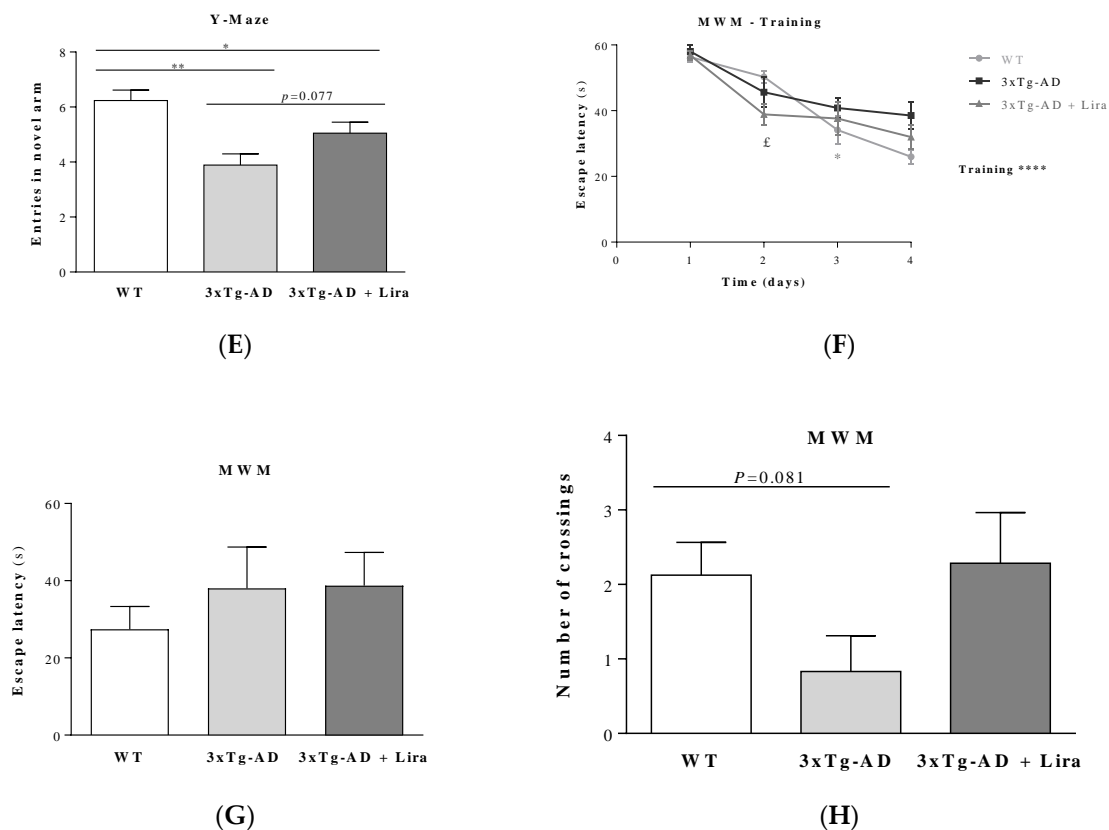


Figure 2. Effect of liraglutide on behavioral performance in female mice with early AD-like pathology. Total distance travelled (A), and distance travelled (B) and time spent in the center (C) of the open field area during the open field test; time spent in start arm during training (D) and number of entries into the novel arm during testing session (E) in the Y-maze test; escape latency across trainings days (F) and testing session (G), and the number of crossings during testing session (H) of the Morris Water Maze test were assessed. Data are the mean \pm SE from 6–10 mice/group. Statistical significance: * $p < 0.05$ or ** $p < 0.01$, by the one-way ANOVA with the Fisher LSD post-hoc test for multiple comparisons (for a Gaussian distribution: A,B,D,E), or by the non-parametric Mann-Whitney test (for a non-Gaussian distribution: C,G,H). Regarding Figure 2F, statistical significance: * $p < 0.05$ in WT day 3 vs. WT day 2, $^{\text{f}}p < 0.05$ in 3xTg-AD + Lira day 2 vs. 3xTg-AD + Lira day 1, **** $p < 0.0001$ by two-way ANOVA, with the Tukey post-hoc test for multiple comparisons.

These results suggest that our mature 3xTg-AD female mice model an early symptomatic stage of the disease, displaying early AD-like pathology with still limited signs of cognitive deficits.

Peripheral and brain inflammation constitutes another prominent feature of AD [39,40]. In line with this, we observed a massive increase in the pro-inflammatory CRP and IL-1 β markers in plasma from the 3xTg-AD female mice, whereas the anti-inflammatory IL-10 was only slightly decreased (by 34%) compared to WT female mice ($F(2,16) = 2.974$; $p = 0.08$ for plasma CRP levels; for plasma IL-10 levels: $Z = -0.857$, $p = 0.445$ for 3xTg-AD vs. WT mice; for plasma IL-1 β levels: $Z = -2.882$, $p = 0.002$ for 3xTg-AD vs. WT mice; Table 1). Liraglutide treatment tended to normalize the plasma inflammatory markers (for plasma IL-10 levels: $Z = -0.319$, $p = 0.805$ for 3xTg-AD + Lira vs. WT mice; $Z = -1.286$, $p = 0.234$ for 3xTg-AD + Lira vs. 3xTg-AD mice; for plasma IL-1 β levels: $Z = -2.00$, $p = 0.051$ for 3xTg-AD + Lira vs. WT mice; $Z = -1.143$, $p = 0.295$ for 3xTg-AD + Lira vs. 3xTg-AD mice; Table 1). Similar to the well-described neuroinflammation markers in AD patients and animal models [41,42], the brains from 3xTg-AD female mice showed a significant increase in the pro-inflammatory CRP ($F(2,11) = 9.337$; $p = 0.004$) and in the anti-inflammatory cytokine IL-10 levels ($F(2,14) = 2.447$; $p = 0.123$) compared to WT female mice (Figure 3). Liraglutide treatment decreased their brain CRP and IL-10 levels (although the later was not statistically significant) (Figure 3). Unexpectedly, no significant

alterations occurred in IL-1 β levels in the brains from 3xTg-AD female mice (data not shown). These results further reinforce the notion that our 3xTg-AD female mice model an asymptomatic stage of the disease, displaying early AD-like neuropathology without substantial signs of cognitive deficits. This is further supported by the lack of significant alterations in brain weight ($F(2,22) = 0.742$; $p = 0.868$; Table 1) or in pre- and postsynaptic markers between experimental groups (data not shown).

Table 1. Effect of liraglutide administration on peripheral features of female mice with early AD-like pathology.

	WT	3xTg-AD	3xTg-AD + Lira
Body weight (g)	29.1 \pm 1.2 (<i>n</i> = 10) (95% CI: 26.3–31.8)	23.3 \pm 0.6 **** (<i>n</i> = 12) (95% CI: 22.1–24.6)	23.3 \pm 0.4 **** (<i>n</i> = 14) (95% CI: 22.6–24.1)
Brain weight (g)	0.5 \pm 0.01 (<i>n</i> = 7) (95% CI: 0.45–0.51)	0.4 \pm 0.03 (<i>n</i> = 8) (95% CI: 0.36–0.52)	0.5 \pm 0.03 (<i>n</i> = 10) (95% CI: 0.42–0.54)
HbA_{1c} (%)	4.3 \pm 0.2 (<i>n</i> = 10) (95% CI: 3.74–4.84)	4.4 \pm 0.1 (<i>n</i> = 11) (95% CI: 4.17–4.65)	4.4 \pm 0.1 (<i>n</i> = 12) (95% CI: 4.13–4.57)
Occasional glycemia (mg glucose/dL blood)	132.8 \pm 3.3 (<i>n</i> = 9) (95% CI: 125.2–140.3)	121.2 \pm 7.3 (<i>n</i> = 12) (95% CI: 105.2–137.2)	128.1 \pm 10.5 (<i>n</i> = 14) (95% CI: 105.6–150.7)
Fasting glycemia (mg glucose/dL blood)	126.4 \pm 4.7 (<i>n</i> = 9) (95% CI: 115.6–137.7)	110.3 \pm 8.2 (<i>n</i> = 12) (95% CI: 92.4–128.3)	127.6 \pm 6.5 <i>p</i> = 0.073 (<i>n</i> = 14) (95% CI: 113.7–141.6)
Fasting insulin levels (ng/mL plasma)	3.5 \pm 1.5 (<i>n</i> = 10) (95% CI: 0.07–6.97)	2.5 \pm 0.8 (<i>n</i> = 11) (95% CI: 0.72–4.23)	1.3 \pm 0.4 (<i>n</i> = 11) (95% CI: 0.56–2.13)
HOMA-IR	30.2 \pm 13.1 (<i>n</i> = 10) (95% CI: 0.7–59.8)	15.2 \pm 5.0 (<i>n</i> = 11) (95% CI: 4.05–26.37)	11.3 \pm 3.1 (<i>n</i> = 11) (95% CI: 4.37–18.26)
HOMA-β	217.5 \pm 124.23 (<i>n</i> = 8) (95% CI: –76.25–511.26)	262.1 \pm 93.01 (<i>n</i> = 9) (95% CI: 47.60–476.5)	170 \pm 43.33 (<i>n</i> = 10) (95% CI: 72–268)
Estradiol levels (pg/mL plasma)	184.1 \pm 15.1 (<i>n</i> = 7) (95% CI: 147.2–220.9)	230.8 \pm 24.3 <i>p</i> = 0.07 (<i>n</i> = 6) (95% CI: 168.3–293.3)	244.9 \pm 9.5 <i>p</i> = 0.023 (<i>n</i> = 6) (95% CI: 220.3–269.4)
C-Reactive Protein levels (ng/mL plasma)	31.9 \pm 6.1 (<i>n</i> = 6) (95% CI: 16.25–47.51)	74.3 \pm 17.6 * (<i>n</i> = 6) (95% CI: 29.10–119.4)	60.8 \pm 10.7 (<i>n</i> = 7) (95% CI: 34.53–86.98)
IL-10 levels (pg/mL plasma)	551.5 \pm 134.6 (<i>n</i> = 7) (95% CI: 222.1–880.9)	364.6 \pm 81.6 (<i>n</i> = 6) (95% CI: 154.8–574.3)	494.3 \pm 54.5 (<i>n</i> = 7) (95% CI: 361.1–627.6)
IL-1β levels (pg/mL plasma)	43.2 \pm 12.3 (<i>n</i> = 6) (95% CI: 11.66–74.66)	821.6 \pm 400.7 ** (<i>n</i> = 6) (95% CI: –208.3–1852)	355.4 \pm 159.3 <i>p</i> = 0.051 (<i>n</i> = 7) (95% CI: –34.38–745.3)

Data are mean \pm SE of the indicated number of mice/group. Statistical significance: * $p < 0.05$, ** $p < 0.01$ or **** $p < 0.0001$ vs. WT female mice, by the one-way ANOVA with the Fisher LSD post-hoc test for multiple comparisons (for a Gaussian distribution), or by the non-parametric Mann-Whitney test (for a non-Gaussian distribution: occasional glycemia, fasting insulin levels, HOMA-IR, HOMA- β , plasma IL-10 and IL-1 β levels). HbA_{1c}: glycated hemoglobin A_{1c}, HOMA-IR: homeostatic model assessment for insulin resistance, HOMA- β : homeostatic model assessment for β -cell function.

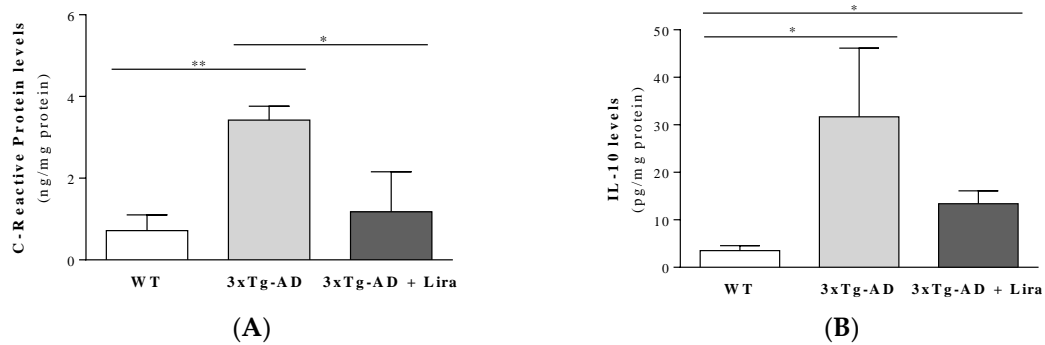


Figure 3. Effect of liraglutide on brain cortical inflammation markers in female mice with early AD-like pathology. Brain cortical C-Reactive Protein (A) and IL-10 (B) were determined. Data are the mean \pm SE from 3–6 mice/group. Statistical significance: * $p < 0.05$ or ** $p < 0.01$, by the one-way ANOVA with the Fisher LSD or Games-Howell post-hoc tests for multiple comparisons.

Other feature of AD is body weight loss [43], whereas peripheral metabolic anomalies remain controversial [44]. Accordingly, our female mice with early AD-like pathology showed a 20% reduction in body weight that, nonetheless, was not recovered by liraglutide treatment ($F(2,33) = 19.7$; $p < 0.0001$; Table 1). Conversely, plasma estradiol levels were slightly increased (between 25–33%) in female mice with early AD-like pathology (treated or not with liraglutide) compared to WT mice ($F(2,16) = 3.568$, $p = 0.052$; Table 1). No significant alterations occurred in the peripheral glucose homeostasis markers occasional ($Z = -0.139$, $p = 0.169$ for 3xTg-AD vs. WT mice; $Z = -0.129$, $p = 0.201$ for 3xTg-AD + Lira vs. WT mice; $Z = -0.129$, $p = 0.899$ for 3xTg-AD + Lira vs. 3xTg-AD mice) and fasting glycemia ($F(2,32) = 1.914$, $p = 0.153$), HbA_{1c} ($F(2,30) = 0.142$, $p = 0.868$), plasma insulin ($Z = -0.352$, $p = 0.756$ for 3xTg-AD vs. WT mice; $Z = -0.07$, $p = 0.973$ for 3xTg-AD + Lira vs. WT mice; $Z = -0.558$, $p = 0.606$ for 3xTg-AD + Lira vs. 3xTg-AD mice), HOMA-IR ($Z = -0.494$, $p = 0.654$ for 3xTg-AD vs. WT mice; $Z = -0.635$, $p = 0.557$ for 3xTg-AD + Lira vs. WT mice; $Z = -0.230$, $p = 0.847$ for 3xTg-AD + Lira vs. 3xTg-AD mice) or HOMA- β ($Z = -1.251$, $p = 0.236$ for 3xTg-AD vs. WT mice; $Z = -0.622$, $p = 0.573$ for 3xTg-AD + Lira vs. WT mice; $Z = -0.572$, $p = 0.604$ for 3xTg-AD + Lira vs. 3xTg-AD mice) between experimental groups (Table 1).

2.2. Liraglutide Partially Normalizes Brain Levels of Estradiol and GLP-1-Related Signaling in Female Mice with Early AD-Like Pathology

AD pathology has been associated with impaired levels and/or activity of hormones and signaling pathways [10,20,45]. Thus, we aimed to analyze the role of peripheral liraglutide treatment on brain estradiol and GLP-1 levels and downstream signaling in female mice with early AD-like pathology.

Similar to the periphery, levels of brain estradiol and GLP-1 were increased in female mice with early AD-like pathology compared to WT ones (for brain GLP-1 levels: $F(2,13) = 2.686$; $p = 0.106$; for brain estradiol levels: $Z = -2.191$, $p = 0.030$ for 3xTg-AD vs. WT mice; Table 2). Liraglutide treatment tended to normalize both estradiol and GLP-1 levels (for brain estradiol levels: $Z = -1.358$, $p = 0.222$ for 3xTg-AD + Lira vs. WT mice; $Z = -0.548$, $p = 0.662$ for 3xTg-AD + Lira vs. 3xTg-AD mice; Table 2). Despite no significant alterations in brain insulin levels nor in IR, GLP-1R or activated Akt between cohorts (data not shown), female mice with early AD-like pathology had a massive decrease in brain active PKA kinase that tended to recover with liraglutide ($Z = -2.562$, $p = 0.009$ for 3xTg-AD vs. WT mice; $Z = -0.548$, $p = 0.662$ for 3xTg-AD + Lira vs. WT mice; $Z = -0.913$, $p = 0.429$ for 3xTg-AD + Lira vs. 3xTg-AD mice; Table 2). These results suggest an impairment in brain GLP-1R-mediated signaling in 3xTg-AD female mice that tended to be normalized by liraglutide administration (Table 2).

Table 2. Effect of liraglutide administration on brain cortical hormones' levels and signaling in female mice with early AD-like pathology.

	WT	3xTg-AD	3xTg-AD + Lira
Estradiol levels (pg/mg protein)	5.62 ± 1.19 (n = 5) (95% CI: 2.31–8.93)	15.2 ± 2.7 * (n = 6) (95% CI: 8.27–22.11)	12.2 ± 3.3 (n = 5) (95% CI: 3.1–21.24)
GLP-1 levels (pg/mg protein)	5.9 ± 2.5 (n = 5) (95% CI: –1.14–12.94)	21.1 ± 6.5 * (n = 6) (95% CI: 4.52–37.74)	15.0 ± 2.8 (n = 5) (95% CI: 7.29–22.76)
Active PKA kinase (ng active PKA/mg protein)	0.01 ± 0.004 (n = 6) (95% CI: –0.0005–0.02)	0.001 ± 0.0004 ** (n = 6) (95% CI: 0.0001–0.002)	0.009 ± 0.005 (n = 5) (95% CI: –0.0048–0.022)

Data are mean ± SE of the indicated number of mice/group. Statistical significance: * $p < 0.05$, ** $p < 0.01$ vs. WT mice, by the one-way ANOVA with the Fisher LSD or Games-Howell post-hoc tests for multiple comparisons (for a Gaussian distribution), or with the non-parametric Mann-Whitney test (for a non-Gaussian distribution: brain estradiol levels and active PKA kinase).

2.3. Liraglutide Promotes Brain Glucose Metabolism via the Oxidative Branch of the Pentose Phosphate Pathway in Female Mice with Early AD-Like Pathology

Another feature of AD is the impairment in brain glucose transport and metabolism [46,47]. Therefore, we next evaluated the effect of liraglutide administration on brain cortical markers for glucose transport and downstream metabolism.

Despite no significant alterations in GLUT4 and GLUT8 expression between experimental groups, brains from female mice with early AD-like pathology had higher glucose levels ($F(2,14) = 2.433$, $p = 0.046$) and slightly increased GLUT1 expression than WT mice (Figure 4A,B). Liraglutide treatment did not significantly affect brain GLUT1 and GLUT4 (an insulin-sensitive glucose transporter; $F(2,13) = 4.491$, $p = 0.033$) or glucose content in early AD-like female mice compared to 3xTg-AD female mice (Figure 4A–C).

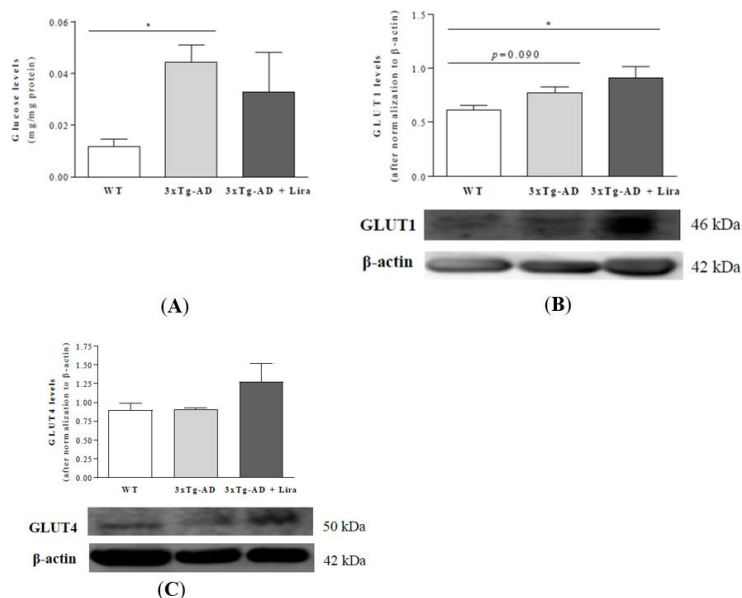


Figure 4. Effect of liraglutide on brain cortical glucose levels and transporters in mature female mice with early AD-like pathology. Brain cortical glucose (A), and GLUT1 (B) and GLUT4 protein levels (C) were evaluated and normalized to β -actin levels, and representative Western blotting images displayed. Data are the mean ± SE from 5–6 mice/group. Statistical significance: * $p < 0.05$, by the one-way ANOVA with the Fisher LSD or Games-Howell post-hoc tests for multiple comparisons.

Moreover, liraglutide abrogated the decrement in the activity of G6PDH (the limiting enzyme from the oxidative branch of the pentose phosphate pathway) in brains from female mice with early AD-like pathology ($Z = -2.309$, $p = 0.029$ for 3xTg-AD vs. WT mice; $Z = -2.309$, $p = 0.029$ for 3xTg-AD + Lira vs. WT mice; $Z = -2.309$, $p = 0.029$ for 3xTg-AD + Lira vs. 3xTg-AD mice; Figure 5A). Regarding glycolysis markers, liraglutide decreased brain pyruvate levels ($F(2,15) = 5.210$, $p = 0.019$) without significant changes in those of lactate in female mice with early AD-like pathology compared to the saline-treated ones (for lactate levels: $Z = 0$, $p = 1$ for 3xTg-AD vs. WT mice; $Z = -0.838$, $p = 0.421$ for 3xTg-AD + Lira vs. WT mice; $Z = -0.548$, $p = 0.662$ for 3xTg-AD + Lira vs. 3xTg-AD mice; Figure 5B,C).

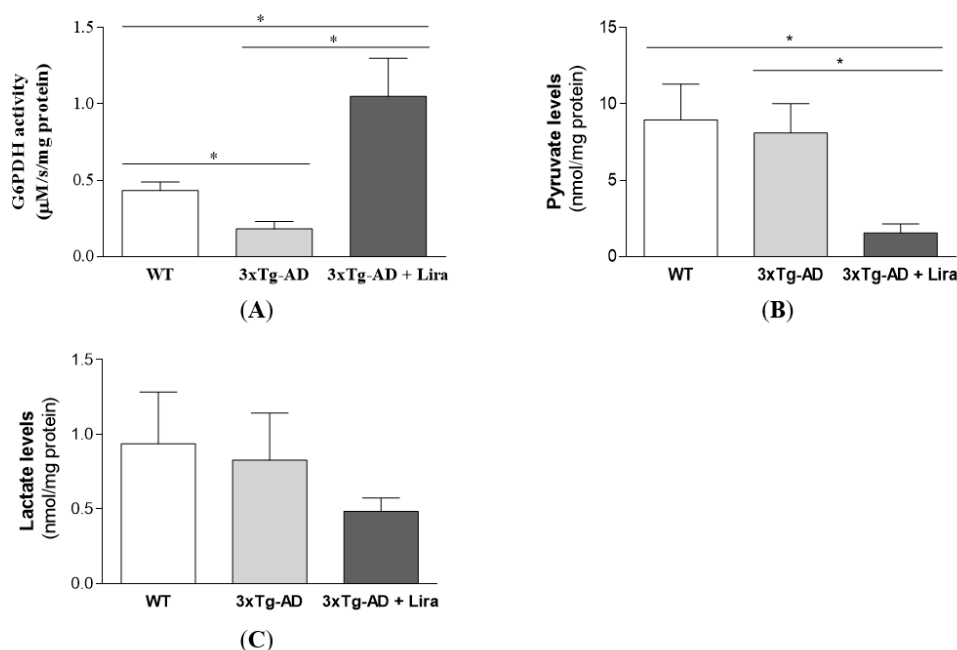


Figure 5. Effect of liraglutide on brain cortical glucose metabolism in female mice with early AD-like pathology. Brain cortical G6PDH activity (A), and pyruvate (B) and lactate levels (C) were determined. Data are the mean \pm SE from 4–6 mice/group. Statistical significance: * $p < 0.05$, by the one-way ANOVA with the Fisher LSD post-hoc test for multiple comparisons (for a Gaussian distribution), or with the non-parametric Mann-Whitney test (for a non-Gaussian distribution: GAPDH activity and lactate levels).

These results suggest that liraglutide-mediated stimulation of G6PDH may be beneficial against brain oxidative stress in female mice with early AD-like pathology.

2.4. Liraglutide Partially Rescues Brain Oxidative/Nitrosative Stress Markers in Female Mice with Early AD-Like Pathology

From the above and since increased oxidative and nitrosative stress was demonstrated in both human and rodent AD brains (including the 3xTg-AD mice) [48,49], we next evaluated the effect of liraglutide on brain oxidative/nitrosative stress markers. Accordingly, brains from female mice with early AD-like pathology showed a slight increase in TBARS (by ~ 1.4 -fold; $F(2,13) = 2.819$, $p = 0.096$; Supplementary Figure S1A) and nitrite levels (by ~ 1.4 -fold; $F(2,15) = 4.30$, $p = 0.033$), and significantly higher carbonyl groups (by ~ 4 -fold; $F(2,14) = 5.755$, $p = 0.015$) and 8-OHdG levels (by ~ 1.9 -fold; $F(2,15) = 3.559$, $p = 0.054$) compared to WT mice (Figure 6A–C). Liraglutide tended to normalize the 8-OH-dG content (Figure 6B), while those of TBARS, carbonyl groups and nitrites were significantly reversed by the drug in female mice with early AD-like pathology (Figure 6A,C; Supplementary Figure S1A).

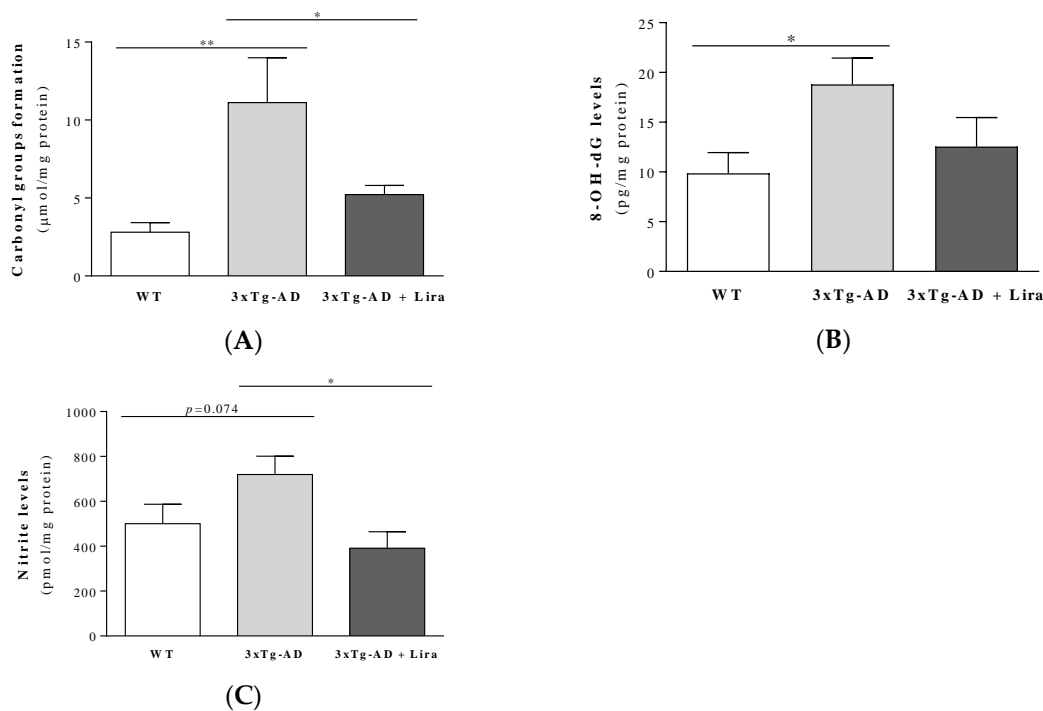


Figure 6. Effect of liraglutide on brain cortical oxidative and nitrosative stress markers in female mice with early AD-like pathology. Brain cortical carbonyl groups formation (A), 8-OH-dG (B) and nitrites levels (C) were determined. Data are the mean \pm SE from 5–7 mice/group. Statistical significance: * $p < 0.05$ or ** $p < 0.01$, by the one-way ANOVA with the Fisher LSD post-hoc test for multiple comparisons.

Recent evidence suggests that, besides its pivotal role in lysosomal-mediated autophagy, p62 may also be involved in oxidative defense, nutrient sensing and inflammation mechanisms [50]. Despite no significant alterations in brain p62 levels in female mice with early AD-like pathology, liraglutide treatment reduced its levels by 20% in these animals ($F(2,15) = 4.424$, $p = 0.031$; Supplementary Figure S1B).

These results suggest that peripheral treatment with liraglutide partially rescued brain oxidative stress markers in female mice with early AD-like pathology.

2.5. Liraglutide Partially Attenuates the Altered Mitochondrial Fission/Fusion Proteins in Female Mice with Early AD-Like Pathology

Alongside the above-mentioned pathophysiological changes in AD, we previously showed alterations in brain mitochondrial dynamics [51]. Therefore, we aimed to study the role of liraglutide on brain markers for mitochondrial fission and fusion. We observed that liraglutide reversed the 2.6-fold increase in Fis1 levels in brains from female mice with early AD-like pathology ($F(2,15) = 5.358$, $p = 0.018$; Figure 7A), while the 1.8-fold lower OPA1 levels were only partially reversed upon liraglutide administration (by 1.6-fold) in female mice with early AD-like pathology ($F(2,15) = 3.636$, $p = 0.052$; Figure 7B).

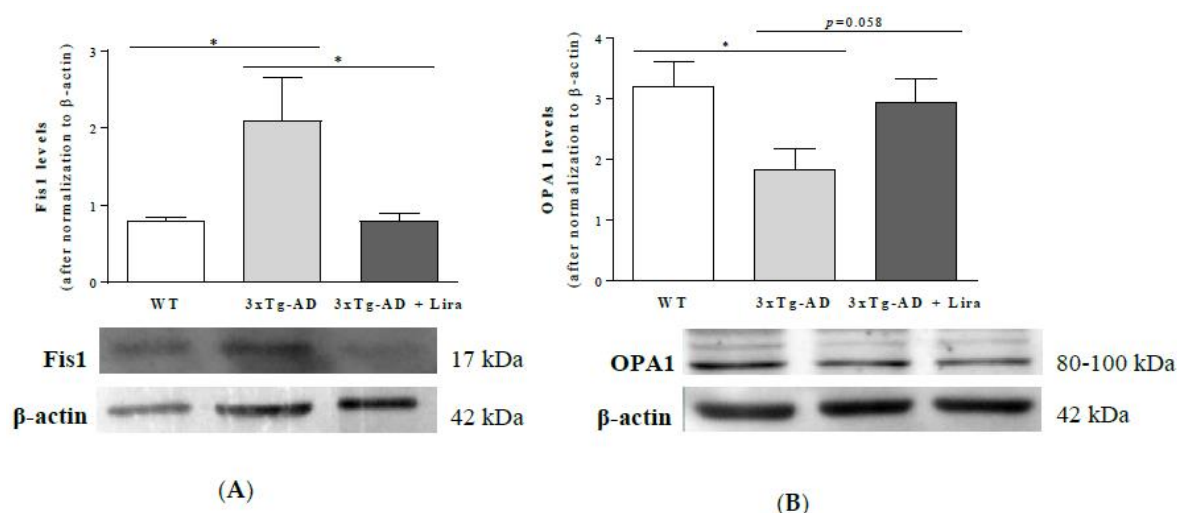


Figure 7. Effect of liraglutide on brain cortical mitochondrial fission/fusion markers in female mice with early AD-like pathology. Brain cortical Fis1 (A) and OPA1 protein levels (B) were determined and normalized to β -actin levels, and representative Western blotting images displayed. Data are the mean \pm SE from 6 mice/group. Statistical significance: * $p < 0.05$, by the one-way ANOVA with the Fisher LSD post-hoc test for multiple comparisons.

These results suggest that peripheral treatment with liraglutide partially attenuated the dysfunctional brain mitochondrial fission/fusion machinery in female mice with early AD-like pathology.

3. Discussion

To the best of our knowledge, this study constitutes a first support to the use of GLP-1 mimetics (namely liraglutide) to mitigate some of the earlier AD-like pathological features in mature females. Contrary to our previous study in 11-month-old 3xTg-AD male mice that showed increased brain cortical and hippocampal A β levels and thigmotaxis, reduced exploratory activity, and deficits in learning and memory [37], in the present study the massive rise in brain cortical A β and p-tau content in 11-month-old 3xTg-AD female mice (in line with the *Amyloid Cascade Hypothesis*—the basis for this mouse model) was accompanied by less pronounced signs of cognitive alterations. Liraglutide treatment only attenuated their increased brain A β_{1-42} levels. This was accompanied by a slight reduction in their plasma and brain inflammatory markers upon liraglutide administration, which also tended to normalize estradiol and GLP-1 content, and PKA-mediated downstream signaling in female mice with early AD-like pathology. Interestingly, liraglutide partially mitigated their brain oxidative stress markers, possibly via the stimulation of G6PDH (and its downstream antioxidant properties) and by altering mitochondrial dynamics, ultimately rescuing the AD-like neuropathology in mature female mice.

Liraglutide administration attenuated memory deficits, A β plaques and oligomers, synaptic and tau pathology in APP/PS1 mice [27] and in non-human primates infused with A β oligomers into the lateral cerebral ventricle [29]. The drug also mitigated the cognitive deficits and cerebral p-tau in diabetic rodents [52,53]. However, others failed to observe a significant effect of chronic liraglutide treatment on cerebral A β plaque formation in two transgenic APP/PS1 mouse models with low and high grade of amyloidosis [54]. This suggested that distinct animal models for AD may display distinct sensitivities to liraglutide treatment [54]. Indeed, a recent study demonstrated that a 2-week administration of liraglutide decreased memory deficits, p-tau and A β overproduction, and increased dendritic spines' density and synaptic proteins upon hyperhomocysteinemia [28]. In this respect, liraglutide injection for 4 weeks only mitigated the brain A β_{1-42} levels, without significantly affecting the A β_{1-40} or p-tau(Ser396) (a known intermediary phosphorylated residue in AD pathology [55,56])

in 3xTg-AD female mice with early AD-like pathology, which also presented less pronounced signs of motor, cognitive or synaptic defects (data not shown) (contrary to the previous observations of impaired motor activity and learning/memory in 3xTg-AD male mice [26,57]). This corroborates the slight delay in the onset of AD-like pathology in 3xTg-AD female mice described by Belfiore et al. [58], together with the notion of a sexual dimorphism in the susceptibility to AD neuropathology, cognitive dysfunction and changes in brain energy metabolism under neuropathological conditions [20,40,59,60] (including the persistently lower metabolic brain age in women across their life span compared to men [61]). Since Yan et al. [62] observed that peripheral 17 β -estradiol treatment activates the estrogen receptor α and the downstream PI3K/Akt/Foxo1 signaling, recovering insulin sensitivity and glucose metabolism, one cannot exclude a role for the increased brain estradiol levels in this delay in AD-like neuropathology in 3xTg-AD female mice (as further discussed by Yang et al. [40]). Accordingly, Yang et al. [40] found that chronic 17 β -estradiol administration to ovariectomized 3xTg-AD female mice recovered their spatial learning and memory, partially due to the recovery of PKA-CREB and downregulation of the p38-MAPK signaling. Hippocampal 17 β -estradiol induced the release of glutamate from astrocytes, stimulating neuronal glutamate receptors, thereby modulating dendritic spine density and growth, and synapse formation and plasticity in developing and adult central nervous system [63,64]. Besides estradiol, the increased brain levels of GLP-1 in female mice with AD-like pathology may constitute an adaptive mechanism to delay the negative effects of less active PKA (its activation by hormones or neurotransmitters in multiple brain regions was shown to regulate feeding, energy expenditure and glucose homeostasis [65–67]). In line with this and with previous studies in AD patients and rodent models (including mature 3xTg-AD male mice) [37,68], our female mice with early AD-like pathology had lower body weight that, contrary to other animal models [69,70], was not recovered by liraglutide treatment.

The delay in AD-like neuropathology in our female 3xTg-AD mice is further supported by their apparently unaltered peripheral glucose metabolism and insulin sensitivity, in contrast with previously studied mature 3xTg-AD male mice [57]. Although it is well-known that metabolic disorders (such as insulin resistance, T2D and/or obesity) increase the risk for AD [38,57,71–74], the opposite (i.e., AD-induced peripheral glucose dysmetabolism and insulin insensitivity) remains a matter of debate [75,76]. This does not invalidate the repurpose of anti-type 2 diabetes drugs to prevent or delay AD progression. Indeed, increasing evidence demonstrates the beneficial effects of, e.g., GLP-1 mimetics (including liraglutide) against AD [18–20]. Among them, we emphasize the liraglutide-induced recovery of brain glucose metabolism (whose changes may start before the onset of brain atrophy and neurodegeneration) [77–83]. Although the precise nature of such metabolic improvement remains unknown, evidence suggests a role for the recovered neurovascular unit (involving a NF- κ B-induced balance between the vasoconstrictor endothelin-1 and the vasodilator endothelial nitric oxide synthase (eNOS)) [84,85] and the normalization of (cerebral) blood flow on the increment of GLUTs levels and/or function (their loss, particularly of those at the blood-brain barrier, like GLUT1 and, to a lesser extent, GLUT4, constitutes an early event in AD pathology) [86,87]. In addition, liraglutide-induced slowdown in brain glucose clearance may aid in the brain recovery of glucose uptake and/or metabolism (as our observations appear to partially confirm), ultimately, in improved cognitive performance [82,86,88–92]. However, others described that the tendentious increase in brain glucose metabolism induced by liraglutide upon AD was not accompanied by a rescue in cognitive function [19,93]. Hopefully, this apparent discrepancy will be clarified by a phase IIb trial involving the treatment of AD individuals with very mild dementia with liraglutide for 12-month (the ELAD trial) [77].

Oxidative/nitrosative stress and inflammation have been also widely demonstrated at the periphery [94–97] and in brains [49,98–100] of human subjects and rodent models of AD [40,48,101,102]. Several authors suggested that impaired redox status, A β deposition, neurofibrillary tangles and neuronal damage [103,104] play a key role in AD pathogenesis, most likely by activating microglia and inflammation-mediated neurotoxicity [105,106]. Accordingly, our female mice with early AD-like

pathology had increased oxidative stress and serum and brain CRP and IL-1 β levels. Indeed, high IL-1 β levels occurred in AD patients and in mild cognitive impaired subjects [107,108], and activated microglia and astrocytes were recently correlated with the levels of hippocampal A β and p-tau, and the severity of AD pathology in 3xTg-AD mice [40]. This hippocampal Tau hyperphosphorylation may arise from an upregulation of the p-38-MAPK cascade in AD, while the downregulation of cAMP-PKA-CREB signaling (as partially observed in Table 2) may impair synaptic plasticity and memory formation [40]. Importantly, the role of the anti-inflammatory cytokine IL-10 in AD brain remains controversial, since recent studies in APP mice suggested that it may inhibit microglial A β clearance, promoting A β plaque generation and cognitive impairment (rather than delaying AD progression) [109]. Furthermore, brain immunity was improved in IL-10-deficient APP mice that also showed lower cerebral amyloidosis [110]. Hence, the increased brain IL-10 content in female mice with early AD-like pathology appears to precede their typical behavioral deficits, possibly exacerbating the brain damage elicited by IL-1 β , CRP and oxidative/nitrosative stress and allowing AD progression. In line with previous studies [27,111], liraglutide partially mitigated brain oxidative stress and inflammation markers in female mice with early AD-like pathology.

Similar to liraglutide's anti-inflammatory mechanisms, those underlying its anti-oxidative stress properties remain poorly understood. These may involve the activation of Akt and eNOS, with the subsequent stimulation of antioxidant defenses (e.g., glutathione, catalase, superoxide dismutase) and reduction of reactive oxygen species (ROS) formation, as observed in ischemic stroke [112,113]. Despite no significant alterations in active Akt in our conditions, one cannot exclude the involvement of the parallel MAPK/ERK signaling cascade [112], known to mediate its antioxidant, anti-inflammatory, anti-apoptotic and pro-cognition roles [114–121], as well as its benefits in AD symptoms and features [77]. Liraglutide-mediated NF- κ B inhibition and Sirt1 may also recover mitochondrial membrane integrity and complex I activity, improving mitochondrial function (as reported in epilepsy, ischemia or toxin exposure) [18,112,122–129], and further protecting against oxidative stress [112,118,130,131], which may also rely on the inhibition of myeloperoxidase (via Nrf2/heme oxygenase-1 downregulation of NADPH oxidase or PKC α membrane translocation, as reported in diabetic and stroke brain) [132]. Importantly, the lower G6PDH activity (a pivotal enzyme from the oxidative branch of the pentose phosphate pathway also involved in the regulation of nicotinamide adenine dinucleotide phosphate (NADPH) and of the key antioxidant reduced glutathione, GSH) observed in brains from female mice with early AD-like pathology further support an increased oxidative stress, in agreement with the G6PDH inhibition in *postmortem* hippocampal regions [133] and prefrontal cortex synaptosomes [134] from AD human subjects. The liraglutide-mediated increase in G6PDH activity and decreased pyruvate levels in mature female mice with early AD-like pathology suggest that its antioxidant effects may involve the stimulation of the oxidative branch of the pentose phosphate pathway (rather than glycolysis) and/or a decrement in p62 levels. Since the liraglutide-induced changes in this stress-inducible protein were not accompanied by alterations in other autophagy markers (p62 is mostly known as a cargo receptor for the lysosomal-mediated autophagy degradation of detrimental and unnecessary components), we hypothesize that p62 may alternatively account for liraglutide's anti-oxidative stress or anti-inflammatory properties. Indeed, p62 was recently associated with Nrf2, mTORC1 and NF- κ B signaling pathways and their role in oxidative stress, nutrient sensing and inflammation [50]. Besides the liraglutide's anti-inflammatory mechanisms discussed above, NF- κ B inhibition was also found to reduce TNF α , IL-1 β and IL-6 levels, and activated microglia and astrocytes [25,123,135–138], while the downregulation of JNK and phosphorylated p38, and the consequent inhibition of caspases-8 and -3, may account for its anti-apoptotic actions [112,115,139,140].

The increased Fis1 and decreased OPA1 levels in female mice with early AD-like pathology suggest a dysregulation in brain mitochondrial fission/fusion machinery, namely the promotion of fission and the impairment of fusion processes [141–143], respectively. OPA1 at the mitochondrial inner membrane is also involved, e.g., in the maintenance of mitochondrial respiratory chain and membrane potential [144], cristae organization, mitochondrial DNA and apoptosis regulation [145–147], whereas

Fis1 can also regulate the size and distribution of mitochondria in response to the local demand for ATP or calcium [148]. Hence, changes in brain OPA1 and Fis1 levels in female mice with early AD-like pathology may elicit alternative damaging mechanisms that were partially reversed by liraglutide.

Although not studied herein, the anti-amyloidogenic/tauogenic effects of liraglutide may also rely on the PI3-K/MAPK/cAMP/PKA-mediated activation of brain insulin degrading enzyme (IDE) and/or the upregulation of A β transporters to promote A β trafficking and proteolytic degradation [149–154]; on the inactive caspase-3-mediated blunt of neurofibrillary tangle formation [112,155–157]; on the regulation of brain neurotransmission (e.g., GABAergic and glutamatergic) [158–163], thus promoting synaptic plasticity; on the improvement of axonal sprouting and neurite outgrowth [130,164–166]; and/or on increased neurogenesis [21,30,136,167–169], ultimately contributing to (AD) brain repair and cognitive function [130,170–172]. Finally, in spite of the apparent lack of changes in the present study, we cannot underestimate the indirect peripheral effects of liraglutide in restoring insulin action and glucose homeostasis, as well as in blood pressure, body weight and lipid profiles [25,30,160,173–181].

Altogether, our results constitute a first approach to disentangle the complex puzzle underlying the use of the GLP-1 mimetic liraglutide as a potential preventive/therapeutic agent against some of the earlier AD-like pathological signs in female mice. Although further studies are needed (particularly in rodent models displaying risk factors for sporadic AD, including aging or diabetes), the different patterns in AD-related pathology between males and females and their response to medicines also reinforce the need for a more tailored, sex/gender-based medicine.

4. Material and Methods

4.1. Materials

Bovine serum albumin (BSA), phenylmethylsulfonyl fluoride (PMSF), dithiothreitol (DTT), Tween 20, thiobarbituric acid (TBA) and mouse monoclonal β -actin (#A5441) antibody were obtained from Sigma-Aldrich (St. Louis, MO, USA). Polyvinylidene difluoride (PVDF) Immobilon-P membranes and rabbit polyclonal glucose transporter 1 (GLUT1, #CBL242) antibody were obtained from Millipore (Billerica, MA, USA). Mouse monoclonal GLUT4 antibody (#2213S) was obtained from Cell Signaling (Leiden, The Netherlands). Mouse monoclonal OPA1 antibody (#612607) was obtained from BD Biosciences (Oeiras, Portugal). Rabbit polyclonal mitochondrial fission 1 protein (Fis1, #NB100-56646) antibody was obtained from Novus Biologicals (Abingdon, United Kingdom). Anti-mouse and anti-rabbit secondary antibodies (#RPN5781 and #RPN5783), and enhanced chemifluorescence (ECF) reagent were purchased from Amersham Biosciences (Little Chalfont, UK). Rat Insulin Enzyme Immunoassay kit (#A05105) was purchased from SPI-BIO, Bertin Pharma (Montigny le Bretonneux, France). Estradiol EIA kit (#582251) and 8-hydroxy-2-deoxy guanosine EIA (#589320) kit were purchased from Cayman Chemical (Ann Arbor, USA). QuantiChrom Glucose Assay kit (#DIGL-100) was purchased from BioAssay Systems (Hayward, CA, USA). Rat Amyloid Beta Peptide 1–42 ELISA kit (#LTI KMB3441) was purchased from EIAab Science Co. (Wuhan, China). Mouse β Amyloid 1–40 ELISA kit (#LTI KMB3481) and Tau [pS396] Human ELISA Kit (#LTI KHB7031) were purchased from Invitrogen (Camarillo, CA, USA). Trichloroacetic acid (TCA) was purchased from Calbiochem (Merck KGaA, Darmstadt, Germany). Rat GLP-1 ELISA Kit (#E-EL-R0059) was purchased from Elabscience (Wuhan, Hubei, China). Rat C-Reactive Protein (CRP) ELISA Kit (#88-7501-28), Rat interleukin (IL)-1 β Platinum ELISA kit (#BMS630) and Rat IL-10 Platinum ELISA kit (#BMS629) were purchased from eBioscience (Vienna, Austria). Protein kinase A (PKA) kinase activity kit (#ADI-EKS-390A) was purchased from Enzo Life Sciences, Grupo Taper SA (Sintra, Portugal). All other chemicals used were of the highest grade of purity commercially available.

4.2. Animal Housing and Treatment

Following EU and Portuguese legislation (Directive 2010/63/EU; DL113/2013, August 7th) and ARRIVE guidelines [182], 10 month-old WT (control) and 3xTg-AD female mice (a genetic model

for AD that develops an age-related progressive neuropathological phenotype) [57] were used upon ethical approval by the Animal Welfare Committee of the Center for Neuroscience and Cell Biology and Faculty of Medicine, University of Coimbra (Project ORBEA_61_2013/24072013). Following the “3Rs” Reduction principle established by FELASA, in a first approach we used the brain cortical GLP-1 levels of saline-treated WT and 3xTg-AD female mice (Table 2) to estimate the number of animals required for this study. Briefly, by using the Wilcoxon-Mann-Whitney test applied to their independent means and standard deviations on the G-Power software [183], an alpha error of 0.05 and a power of 80%, we estimated that a total of six mice should be used for the overall study. In line with this and aiming to increase the power of our hypothesis, we used a minimum of four mice per parameter.

Mice were maintained at our animal colony (Animal Research Center, University of Coimbra) in static microisolator cages (3–4 mice/cage) with a filter top and bedding and nesting materials, under controlled light (12h day/night cycle) and humidity (45–65%) and *ad libitum* standard hard pellets chow and sterilized and acidified water (pH 2.5–3). Signs of distress were carefully monitored. Mice were randomly divided into three experimental groups: in the first one, 14 3xTg-AD female mice were daily, subcutaneously (s.c.) injected with liraglutide (0.2mg/kg), for 28 days, whereas the remaining two groups (10 wild type and 12 3xTg-AD mice; mice with AD-like pathology were subjected to random assignments) received saline injection (0.9% sterile NaCl). Although not expected, a rapid decrease in body weight >15–20% was defined as a humane endpoint for the study.

4.3. Body and Brain Weight

Body weight was monitored once/week throughout the study. Immediately before euthanasia, animals were also weighed. After euthanasia, brains were immediately removed and weighed. Results were expressed as body weight or brain weight (g).

4.4. Collection of Peripheral Blood and Routine Biochemical Analyses

Mice were fasted for ~6h (starting early in the morning) and immediately after their euthanasia blood was immediately collected directly from the heart by transcardial puncture to commercially-available blood collection tubes containing EDTA (Vacuette® K3E/EDTA3K; Greiner Bio One, Kremsmünster, Austria) to isolate plasma (as detailed below). One drop of blood was used to determine fasting or occasional blood glucose levels by the glucose oxidase reaction, using a glucometer (Glucometer-Elite, Bayer SA, Portugal) and compatible stripes. Results were expressed as mg glucose/dL blood.

Blood glycated hemoglobin (HbA_{1c}) was measured with the Multi-Test HbA_{1c} (A1C Now+, Bayer SA, Portugal) and results expressed as %. The remaining blood was centrifuged at 572× *g* for 10 min, at 4 °C, in a Sigma 2–16 PK centrifuge. The resulting plasma was used to determine fasting insulin levels through the Insulin Enzyme Immunoassay kit, according to the manufacturer’s instructions. Absorbance was read at 405 nm in a SpectraMax Plus 384 multiplate reader, when maximum binding (B₀) wells reached 0.2–0.8 arbitrary units (a.u.) Results were expressed as ng/mL plasma.

Plasma estradiol levels were measured by the Estradiol EIA kit, according to the manufacturer’s instructions. Absorbance was read at 450 nm, in a SpectraMax Plus 384 multiplate reader. Results were expressed as pg/mL plasma.

4.5. Isolation and Preparation of Brain Cortical Homogenates

After euthanasia, brains were immediately removed and cortices dissected and snap-frozen for further studies. Brain cortices were then homogenized at 0–4 °C in lysis buffer, containing (in mM): 25 HEPES, 2 MgCl₂, 1 EDTA, 1 EGTA, pH 7.4, supplemented with 2 mM DTT, 100 μM PMSF and commercial protease and phosphatase inhibitors cocktails. The crude homogenate was centrifuged at 17,968× *g* for 10 min, at 4 °C in a Sigma 2–16K centrifuge to remove the nuclei, and the resulting supernatant was collected. Pellet was further resuspended in supplemented buffered solution and centrifuged again at 17,968× *g* for 10 min, at 4 °C. The supernatant was added to the

previously obtained one and protein content determined by the Bio-Rad Protein Assay, according to the manufacturer's instructions.

4.6. Evaluation of AD Pathological Hallmarks

Brain cortical $A\beta_{1-42}$ levels were determined in 10 μ L brain cortical homogenates by the Amyloid Beta Peptide 1–42 ELISA kit, according to the manufacturer's instructions. Absorbance was determined at 450 nm, in a SpectraMax Plus 384 multiplate reader. Results were expressed as pg/mg protein.

Brain cortical $A\beta_{1-40}$ levels were determined in 10 μ L of brain cortical homogenates by the β -Amyloid 1–40 ELISA kit, according to the manufacturer's instructions. Absorbance was determined at 450 nm, in a SpectraMax Plus 384 multiplate reader. Results were expressed as pg/mg protein.

Brain cortical levels of p-tau protein at the serine 396 residue (Tau pSer396) were determined in 10 μ L of brain cortical homogenates by the Tau [pS396] Human ELISA Kit, according to the manufacturer's instructions. Absorbance was read at 450 nm in a SpectraMax Plus 384 multiplate reader. Results were expressed as pg/mg protein.

4.7. Behavioral Analyses

At the end of treatment, mice were transported in their home cages to the behavioral testing room and allowed to acclimate to the room for at least 2h prior to each test. Behavioral tests were performed in consecutive days, by experienced observers blind to the experimental conditions.

4.7.1. Open Field Behavior Test

Open field behavior testing allows the assessment of the locomotor and behavioral activity in rodents [184]. Motor activity was evaluated during night cycle in an open field squared arena with grey open-topped boxes (50 cm wide \times 50 cm deep \times 40 cm high), using the Stoelting ANY-MAZE video tracking system (Stoelting Co., Wood Dale, IL, USA), detecting position of the animal's head. Mice were placed individually in the corner of the open field arena and were recorded for a 30-min period. Data were collected every 5 min.

4.7.2. Y-maze Behavior Test

Short-term spatial memory was evaluated using the modified Y-maze test, based on the innate preference of animals to explore areas that have not been previously explored [185]. Briefly, using a Y-shaped plexiglass apparatus consisting of three arms (18 cm long, 6 cm wide and 6 cm high) separated by equal angles, mice were subjected to a training session whereby they freely explored two arms (Start and Other) for 8 min, while the third one (Novel) was blocked [186–188]. After a 120-min inter-trial interval, mice were subjected to the test session, after the removal of the wall that blocked the Novel arm and its opening for free exploration of the three arms for 8 min. Memory performance was given by the percentage of time spent in the novel arm over the time spent exploring all arms.

4.7.3. Morris Water Maze Test

Spatial memory was assessed by the Morris water maze (MWM) test, as described by Morris et al. [189], with slight modifications [185]. Briefly, tests were performed in a circular swimming pool made of grey-painted fiberglass, 1.2 m inside diameter, 0.8 m high, which was filled to a depth of 0.6 m with water maintained a 23 ± 2 °C. The target platform (10 \times 10 cm²) of transparent acrylic resin was submerged 1–1.5 cm beneath the water surface and it was cued by a 7-cm diameter white ball attached to the top of the platform and protruding above the water. Starting points were marked on the outside of the pool as north (N), south (S), east (E) and west (W). Four distant cues (55 \times 55 cm²) were placed 30 cm above the upper edge of the water tank and the position of each symbol marked the midpoint of the perimeter of a quadrant (circle = NE quadrant, square = SE quadrant, cross = SW

quadrant and diamond = NW quadrant). A monitor and a video-recording system were installed in an adjacent room.

Mice were submitted to a cued version of the water maze [190], consisting of four training days and four consecutive trials per day, during which the animals were left in the tank facing the wall and were then allowed to swim freely to the submerged platform placed in the center of one of the four imaginary quadrants of the tank. The initial position in which the animal was left in the tank was one of the four vertices of the imaginary quadrants of the tank, by the following order: north, south, east and west. If the mouse did not find the platform during a period of 60 s, it was gently guided to it. After the animal had escaped to the platform, it remained on it for 10 s and was then removed from the tank for 20 s before being placed in the next random initial position. Test session (day five) consisted of a single trial, in which the platform was removed and each mouse was allowed to swim for 60 s in the maze. The experiments were recorded and the scores for latency of escape from the starting point to the platform and swimming speed were later measured with the ANY-MAZE™ video tracking system.

4.8. Evaluation of Inflammation Markers

Inflammation markers were evaluated in plasma and brain cortical homogenates, by using the C-Reactive Protein (CRP) ELISA Kit, IL-10 Platinum ELISA kit and IL-1 β Platinum ELISA kit, according to the manufacturer's instructions. Briefly, 7.5 μ L of plasma and 5 μ L of each brain cortical homogenate were used to determine CRP levels, whereas 10 μ L of plasma and each brain cortical homogenate were used for IL-10 and IL-1 β levels. Absorbance was read at 450 nm, in a SpectraMax Plus 384 multiplate reader. Results were expressed as ng/mL plasma and ng/mg protein for CRP, and as pg/mL plasma and pg/mg protein for IL-1 β and IL-10.

4.9. Evaluation of Brain Cortical Hormones' Levels

Brain cortical estradiol levels were measured in 10 μ L of each sample (with the remaining volumes decreased to half) by using the Estradiol EIA kit, according to the manufacturer's instructions. Absorbance was determined by a SpectraMax Plus 384 multiplate reader, at 450 nm. Results were expressed as pg/mg protein.

Brain cortical GLP-1 levels were measured in 20 μ L of each sample (working dilution of 1:5) by the Rat GLP-1 ELISA Kit. Absorbance was determined at 450 nm, in a SpectraMax Plus 384 multiplate reader. Results were expressed as pg/mg protein.

4.10. Assessment of Brain Cortical PKA Activity

Active PKA kinase was determined in 5 μ L of each sample (working dilution of 1:6) by the PKA kinase activity kit. Absorbance was determined at 450 nm, in a SpectraMax Plus 384 multiplate reader. Results were expressed as ng/mg protein.

4.11. Assessment of Brain Cortical Glucose Levels

Brain cortical glucose levels were determined by the QuantiChrom™ Glucose Assay kit, according to the manufacturer's instructions, in 5 μ L of each brain cortical homogenate. Absorbance was read at 630 nm, in a SpectraMax Plus 384 multiplate reader. Results were expressed as mg/mg protein.

4.12. Determination of Brain Markers for Glycolysis and Pentose Phosphate Pathway

Glycolytic metabolism and pentose phosphate pathways were given by the activity of the pentose phosphate pathway enzyme G6PDH, and by the levels of pyruvate and lactate in mouse brain cortical lysates.

Pentose phosphate pathway was given by the activity of G6PDH, that catalyzes the formation of 6-phosphogluconolactone from G6P, at the expense of NADP⁺, according to a previously described method [191]. Briefly, 5 μ L of each brain cortical lysate were incubated in a reaction buffer containing

50 mM Tris-HCl (pH 7.5) and supplemented with 50 μM MgCl_2 and 7.2 μM NADP^+ . Absorbance was read at 340nm, at 37 °C, during 2 min, with readings of 20 s intervals, in a SpectraMax Plus 384 microplate reader. Then, the reaction was initiated by the addition of 0.5 mM G6P, and the absorbance continuously read for 150 s, with 20 s intervals. G6PDH activity was calculated using a $\epsilon_{340\text{ nm}} = 6220\text{ M}^{-1}\text{cm}^{-1}$. Results were expressed as $\mu\text{M/s/mg}$ protein.

Pyruvate levels were determined by the Pyruvate Colorimetric/Fluorometric assay kit, according to the manufacturer's instructions, in 5 μL of brain cortical lysate (working dilution 1:10). Absorbance was read at 570 nm, in a SpectraMax Plus 384 microplate reader. Results were expressed as nmol/mg protein.

Lactate levels were determined by the Lactate Colorimetric/Fluorometric assay kit, according to the manufacturer's instructions, in 5 μL of each brain cortical homogenate (working dilution 1:10). Absorbance was read at 570 nm, in a SpectraMax Plus 384 microplate reader. Results were expressed as nmol/mg protein.

4.13. Evaluation of Oxidative/Nitrosative Stress Markers

Carbonyl groups were determined according to Fagan et al. [192], with slight modifications. Briefly, 5 μL of each brain cortical homogenate were dissolved in 71 μL TCA 20%, and centrifuged at $9167\times g$, for 3 min, in a Sigma 2–16K centrifuge. The pellet obtained was incubated for 1h, at room temperature, in 35 μL DNPH 10 mM (freshly prepared in 2M HCl) protected from light and with vortex agitation every 10min. Then, 35 μL TCA 20% were added and the mixture was centrifuged at $11,092\times g$, for 3 min. The resulting pellet was mixed with 71 μL ethanol:ethyl acetate (1:1, *v/v*), and centrifuged again at $9167\times g$, for 3 min. Then, the pellet was incubated in 64.3 μL guanidine 6M (prepared in PBS, pH 6.5), for 15 min, at 37 °C, and centrifuged at $9167\times g$ for 3 min. For all samples, a blank was prepared, which was incubated with HCl 2M instead of DNPH. Carbonyl content was calculated from the maximum absorbance, at 360 nm, measured in a SpectraMax Plus 384 multiplate reader, and an $\epsilon_{360\text{ nm}} = 22 \times 10^3\text{ M}^{-1}\text{cm}^{-1}$. The results were expressed as $\mu\text{mol/mg}$ protein.

Levels of the DNA oxidation marker 8-hydroxy-2-deoxy guanosine (8-OH-dG) were determined in 10 μL of brain cortical homogenates by the 8-OH-dG EIA kit (Cayman Chemical Co.), according to the manufacturer's instructions. Absorbance was read at 405 nm, in a SpectraMax Plus 384 multiplate reader. Results were expressed as pg/mg protein.

Nitrite levels were indirectly given by the NO^\bullet production upon the reaction with Griess reagent, according to Green et al. [193]. Briefly, 100 μg of each brain cortical homogenate were diluted in 100 μL phosphate buffer and incubated, for 10 min, in 100 μL Griess reagent (containing 1% sulfanilamide in 2.5% phosphoric acid, plus 0.1% *N*-(1-naphthyl) ethylenediamine dihydrochloride), protected from light. Absorbance was read at 550nm, in a SpectraMax Plus 384 multiplate reader. Nitrite content was calculated using a standard curve of sodium nitrite. Results were expressed as pmol/mg protein.

4.14. Western Blot Analyses

Samples containing denatured brain cortical homogenates (50 μg per lane) were subjected to sodium dodecyl sulfate (SDS)/polyacrylamide gel electrophoresis (SDS/PAGE) (8–15%) and transferred onto polyvinyl difluoride (PVDF) membranes. Then, membranes were blocked for 1h at room temperature in Tris-buffered saline (TBS, pH 7.4) plus 1% or 5% BSA and 0.05% Tween 20. Membranes were then incubated overnight at 4°C with rabbit GLUT1 (1:1000), mouse GLUT4 (1:1000), rabbit Fis1 (1:750) and mouse OPA1 (1:1000) primary antibodies. Membranes were then incubated with the respective anti-rabbit or -mouse secondary IgG antibodies (1:10,000), for 2h, at room temperature, and developed using ECF. Immunoreactive bands were visualized by the VersaDoc Imaging System (Bio-Rad, Hercules, CA, USA). Fluorescence signal was analyzed using the QuantityOne software and the results given as INT/ mm^2 . Of note, membranes were then reprobed with the corresponding mouse β -actin (1:5000) primary antibody. Results were presented as the ratio between total protein vs. β -actin.

4.15. Statistical Analysis

Authors performed the statistical analysis using SPSS version 24.0 (IBM Corp., Armonk, NY, USA). The extreme outliers were discarded, based on the 3× IQR criterion. The Shapiro-Wilk test was used to assess the normality of data ($p > 0.05$), since the number of mice/group were considered small (i.e., $n < 50$). The normally distributed data were evaluated concerning the homogeneity of variance, using the Levene's test ($p > 0.05$). For data with a Gaussian distribution, a parametric one-way analysis of variance (ANOVA) was performed to determine whether there were significant overall differences ($p < 0.05$) between the mean of more than two groups. To determine which groups differed from the rest ($p < 0.05$), the Fisher's Least Significant Difference (LSD), Bonferroni or the Games-Howell *post-hoc* tests were used. For data with a non-Gaussian distribution, a non-parametric Mann-Whitney test was used ($p < 0.05$). In this study, the groups analyzed were the brain cortical homogenates, blood or plasma from mature female WT mice, 3xTg-AD and 3xTg-AD + Liraglutide mice. Statistical significance was defined as $p < 0.05$.

Graphic artwork was obtained using the GraphPad Prism 6.0 software (GraphPad Software, San Diego, CA, USA). Data were presented as mean \pm SE of the indicated number of mice/group, run in duplicate.

Supplementary Materials: Supplementary materials can be found at <http://www.mdpi.com/1422-0067/21/5/1746/s1>.

Author Contributions: A.I.D., E.C., I.N.A., D.M., D.F.S. and E.J.C. performed the experiments and data analyses. Behavioral experiments: A.I.D., E.C. and N.J.M. Manuscript writing: A.I.D. and P.I.M. Experimental design, data analysis, and discussion: A.I.D., E.C., N.J.M., E.J.C., M.S.S., C.R.O. and P.I.M. All authors have read and agreed to the published version of the manuscript.

Funding: This work was supported by the European Regional Development Fund (ERDF), through the Centro 2020 Regional Operational Programme (Projects Healthy Aging2020, Centro-01-0145-FEDER-000012; PTDC/SAU-TOX/117481/2010); by COMPETE 2020 (Operational Programme for Competitiveness and Internationalization); by Portuguese national funds via FCT – Fundação para a Ciência e a Tecnologia (projects: PTDC/SAUTOX/117481/2010; UIDB/NEU/04539/2020; and by the European Social Fund (Fellowship SFRH/BD/90036/2012 to E. Candeias and Post-Doctoral Researcher Contract DL57/2016 #SFRH/BPD/84473/2012 to A. I. Duarte).

Acknowledgments: We are grateful to Rodrigo Cunha (CNC and Laboratory of Biochemistry, Faculty of Medicine, University of Coimbra, Coimbra, Portugal) for his valuable help with the behavioral tests.

Conflicts of Interest: The authors declare no conflict of interest. The funders had no role in the design of the study; in the collection, analyses or interpretation of data; in the writing of the manuscript, or in the decision to publish the results.

References

1. Grundke-Iqbal, I.; Iqbal, K.; Tung, Y.C.; Quinlan, M.; Wisniewski, H.M.; Binder, L.I. Abnormal phosphorylation of the microtubule-associated protein tau (τ) in Alzheimer cytoskeletal pathology. *Proc. Natl. Acad. Sci. USA* **1986**, *83*, 4913–4917. [[CrossRef](#)]
2. Glenner, G.G.; Wong, C.W. Alzheimer's disease: Initial report of the purification and characterization of a novel cerebrovascular amyloid protein. *Biochem. Biophys. Res. Commun.* **1984**, *120*, 885–890. [[CrossRef](#)]
3. Lopera, F. Clinical features of early-onset Alzheimer disease in a large kindred with an E280A presenilin-1 mutation. *J. Am. Med. Assoc.* **1997**, *277*, 793–799. [[CrossRef](#)]
4. Brookmeyer, R.; Gray, S.; Kawas, C. Projections of Alzheimer's disease in the United States and the public health impact of delaying disease onset. *Am. J. Public Health* **1998**, *88*, 1337–1342. [[CrossRef](#)] [[PubMed](#)]
5. Farrer, L.A.; Cupples, L.A.; Haines, J.L.; Hyman, B.; Kukull, W.A.; Mayeux, R.; Myers, R.H.; Pericak-Vance, M.A.; Risch, N.; Van Duijn, C.M. Effects of age, sex, and ethnicity on the association between apolipoprotein E genotype and Alzheimer disease: A meta-analysis. *J. Am. Med. Assoc.* **1997**, *278*, 1349–1356. [[CrossRef](#)]
6. Sperling, R.; Mormino, E.; Johnson, K. The evolution of preclinical Alzheimer's disease: Implications for prevention trials. *Neuron* **2014**, *84*, 608–622. [[CrossRef](#)]

7. Mosconi, L.; Berti, V.; Guyara-Quinn, C.; McHugh, P.; Petrongolo, G.; Osorio, R.S.; Connaughty, C.; Pupi, A.; Vallabhajosula, S.; Isaacson, R.S.; et al. Perimenopause and emergence of an Alzheimer's bioenergetic phenotype in brain and periphery. *PLoS ONE* **2017**, *12*, e0185926. [[CrossRef](#)]
8. Mosconi, L.; Berti, V.; Quinn, C.; McHugh, P.; Petrongolo, G.; Varsavsky, I.; Osorio, R.S.; Pupi, A.; Vallabhajosula, S.; Isaacson, R.S.; et al. Sex differences in Alzheimer risk: Brain imaging of endocrine vs chronologic aging. *Neurology* **2017**, *89*, 1382–1390. [[CrossRef](#)]
9. Fisher, D.W.; Bennett, D.A.; Dong, H. Sexual dimorphism in predisposition to Alzheimer's disease. *Neurobiol. Aging* **2018**, *70*, 308–324. [[CrossRef](#)]
10. Mosconi, L.; Rahman, A.; Diaz, I.; Wu, X.; Scheyer, O.; Hristov, H.W.; Vallabhajosula, S.; Isaacson, R.S.; de Leon, M.J.; Brinton, R.D. Increased Alzheimer's risk during the menopause transition: A 3-year longitudinal brain imaging study. *PLoS ONE* **2018**, *13*, e0207885. [[CrossRef](#)]
11. Laughlin, G.A.; Kritz-Silverstein, D.; Barrett-Connor, E. Higher endogenous estrogens predict four year decline in verbal fluency in postmenopausal women: The rancho Bernardo study. *Clin. Endocrinol.* **2010**, *72*, 99–106. [[CrossRef](#)] [[PubMed](#)]
12. Li, R.; Cui, J.; Jothishankar, B.; Shen, J.; He, P.; Shen, Y. Early reproductive experiences in females make differences in cognitive function later in life. *J. Alzheimers Dis.* **2013**, *34*, 589–594. [[CrossRef](#)] [[PubMed](#)]
13. Heys, M.; Jiang, C.; Cheng, K.K.; Zhang, W.; Au Yeung, S.L.; Lam, T.H.; Leung, G.M.; Schooling, C.M. Lifelong endogenous estrogen exposure and later adulthood cognitive function in a population of naturally postmenopausal women from southern China: The Guangzhou biobank cohort study. *Psychoneuroendocrinology* **2011**, *36*, 864–873. [[CrossRef](#)] [[PubMed](#)]
14. Colucci, M.; Cammarata, S.; Assini, A.; Croce, R.; Clerici, F.; Novello, C.; Mazzella, L.; Dagnino, N.; Mariani, C.; Tanganelli, P. The number of pregnancies is a risk factor for Alzheimer's disease. *Eur. J. Neurol.* **2006**, *13*, 1374–1377. [[CrossRef](#)] [[PubMed](#)]
15. Sobow, T.; Kloszewska, I. Parity, number of pregnancies, and the age of onset of Alzheimer's disease. *J. Neuropsychiatry Clin. Neurosci.* **2004**, *16*, 120–121. [[CrossRef](#)]
16. Aragno, M.; Mastrocola, R.; Brignardello, E.; Catalano, M.; Robino, G.; Manti, R.; Parola, M.; Danni, O.; Boccuzzi, G. Dehydroepiandrosterone modulates nuclear factor-kappaB activation in hippocampus of diabetic rats. *Endocrinology* **2002**, *143*, 3250–3258. [[CrossRef](#)]
17. Ptok, U.; Barkow, K.; Heun, R. Fertility and number of children in patients with Alzheimer's disease. *Arch. Womens Ment. Health* **2002**, *5*, 83–86. [[CrossRef](#)]
18. Camkurt, M.A.; Lavagnino, L.; Zhang, X.Y.; Teixeira, A.L. Liraglutide for psychiatric disorders: Clinical evidence and challenges. *Horm. Mol. Biol. Clin. Investig.* **2018**, *36*. [[CrossRef](#)]
19. Loera-Valencia, R.; Cedazo-Minguez, A.; Kenigsberg, P.A.; Page, G.; Duarte, A.I.; Giusti, P.; Zusso, M.; Robert, P.; Frisoni, G.B.; Cattaneo, A.; et al. Current and emerging avenues for Alzheimer's disease drug targets. *J. Intern. Med.* **2019**, *286*, 398–437. [[CrossRef](#)]
20. Duarte, A.I.; Santos, M.S.; Oliveira, C.R.; Moreira, P.I. Brain insulin signalling, glucose metabolism and females' reproductive aging: A dangerous triad in Alzheimer's disease. *Neuropharmacology* **2018**, *136*, 223–242. [[CrossRef](#)]
21. De Felice, F.G.; Ferreira, S.T. Inflammation, defective insulin signaling, and mitochondrial dysfunction as common molecular denominators connecting type 2 diabetes to Alzheimer disease. *Diabetes* **2014**, *63*, 2262–2272. [[CrossRef](#)] [[PubMed](#)]
22. Nadkarni, P.; Chepurny, O.G.; Holz, G.G. Regulation of glucose homeostasis by GLP-1. *Prog. Mol. Biol. Transl. Sci.* **2014**, *121*, 23–65. [[CrossRef](#)] [[PubMed](#)]
23. Hamilton, A.; Patterson, S.; Porter, D.; Gault, V.A.; Holscher, C. Novel GLP-1 mimetics developed to treat type 2 diabetes promote progenitor cell proliferation in the brain. *J. Neurosci. Res.* **2011**, *89*, 481–489. [[CrossRef](#)] [[PubMed](#)]
24. Li, L.; Zhang, Z.F.; Holscher, C.; Gao, C.; Jiang, Y.H.; Liu, Y.Z. (Val(8)) glucagon-like peptide-1 prevents tau hyperphosphorylation, impairment of spatial learning and ultra-structural cellular damage induced by streptozotocin in rat brains. *Eur. J. Pharmacol.* **2012**, *674*, 280–286. [[CrossRef](#)] [[PubMed](#)]
25. Gault, V.A.; Holscher, C. GLP-1 agonists facilitate hippocampal LTP and reverse the impairment of LTP induced by beta-amyloid. *Eur. J. Pharmacol.* **2008**, *587*, 112–117. [[CrossRef](#)] [[PubMed](#)]

26. Chen, S.; Sun, J.; Zhao, G.; Guo, A.; Chen, Y.; Fu, R.; Deng, Y. Liraglutide improves water maze learning and memory performance while reduces hyperphosphorylation of Tau and neurofilaments in APP/PS1/Tau triple transgenic mice. *Neurochem. Res.* **2017**, *42*, 2326–2335. [[CrossRef](#)]
27. McClean, P.L.; Parthasarathy, V.; Faivre, E.; Holscher, C. The diabetes drug liraglutide prevents degenerative processes in a mouse model of Alzheimer's disease. *J. Neurosci.* **2011**, *31*, 6587–6594. [[CrossRef](#)]
28. Zhang, Y.; Xie, J.Z.; Xu, X.Y.; Hu, J.; Xu, T.; Jin, S.; Yang, S.J.; Wang, J.Z. Liraglutide ameliorates hyperhomocysteinemia-induced Alzheimer-like pathology and memory deficits in rats via multi-molecular targeting. *Neurosci. Bull.* **2019**, *35*, 724–734. [[CrossRef](#)]
29. Batista, A.F.; Forný-Germano, L.; Clarke, J.R.; Lyra, E.S.N.M.; Brito-Moreira, J.; Boehnke, S.E.; Winterborn, A.; Coe, B.C.; Lablans, A.; Vital, J.F.; et al. The diabetes drug liraglutide reverses cognitive impairment in mice and attenuates insulin receptor and synaptic pathology in a non-human primate model of Alzheimer's disease. *J. Pathol.* **2018**, *245*, 85–100. [[CrossRef](#)]
30. Han, W.N.; Holscher, C.; Yuan, L.; Yang, W.; Wang, X.H.; Wu, M.N.; Qi, J.S. Liraglutide protects against amyloid-beta protein-induced impairment of spatial learning and memory in rats. *Neurobiol. Aging* **2013**, *34*, 576–588. [[CrossRef](#)]
31. Long-Smith, C.M.; Manning, S.; McClean, P.L.; Coakley, M.F.; O'Halloran, D.J.; Holscher, C.; O'Neill, C. The diabetes drug liraglutide ameliorates aberrant insulin receptor localisation and signalling in parallel with decreasing both amyloid-beta plaque and glial pathology in a mouse model of Alzheimer's disease. *Neuromol. Med.* **2013**, *15*, 102–114. [[CrossRef](#)] [[PubMed](#)]
32. Hunter, K.; Holscher, C. Drugs developed to treat diabetes, liraglutide and lixisenatide, cross the blood brain barrier and enhance neurogenesis. *BMC Neurosci.* **2012**, *13*, 33. [[CrossRef](#)] [[PubMed](#)]
33. Andrieu, S.; Coley, N.; Lovestone, S.; Aisen, P.S.; Vellas, B. Prevention of sporadic Alzheimer's disease: Lessons learned from clinical trials and future directions. *Lancet Neurol.* **2015**, *14*, 926–944. [[CrossRef](#)]
34. Masters, C.L.; Bateman, R.; Blennow, K.; Rowe, C.C.; Sperling, R.A.; Cummings, J.L. Alzheimer's disease. *Nat. Rev. Dis. Primers* **2015**, *1*, 15056. [[CrossRef](#)] [[PubMed](#)]
35. Harris, F.; Pierpoint, L. Photodynamic therapy based on 5-aminolevulinic acid and its use as an antimicrobial Agent. *Med. Res. Rev.* **2012**, *32*, 1292–1327. [[CrossRef](#)]
36. Stuss, D.T.; Knight, R.T. *Principles of Frontal Lobe Function*, 2nd ed.; Oxford University Press: New York, NY, USA, 2013.
37. Carvalho, C.; Machado, N.; Mota, P.C.; Correia, S.C.; Cardoso, S.; Santos, R.X.; Santos, M.S.; Oliveira, C.R.; Moreira, P.I. Type 2 diabetic and Alzheimer's disease mice present similar behavioural, cognitive, and vascular anomalies. *J. Alzheimers Dis.* **2013**, *35*, 623–635. [[CrossRef](#)]
38. Serrano-Pozo, A.; Frosch, M.P.; Masliah, E.; Hyman, B.T. Neuropathological alterations in Alzheimer disease. *Cold. Spring Harb. Perspect. Med.* **2011**, *1*, a006189. [[CrossRef](#)]
39. De Luigi, A.; Pizzimenti, S.; Quadri, P.; Lucca, U.; Tettamanti, M.; Fragiaco, C.; De Simoni, M.G. Peripheral inflammatory response in Alzheimer's disease and multiinfarct dementia. *Neurobiol. Dis.* **2002**, *11*, 308–314. [[CrossRef](#)]
40. Yang, J.T.; Wang, Z.J.; Cai, H.Y.; Yuan, L.; Hu, M.M.; Wu, M.N.; Qi, J.S. Sex differences in neuropathology and cognitive behaviour in APP/PS1/tau triple-transgenic mouse model of Alzheimer's disease. *Neurosci. Bull.* **2018**, *34*, 736–746. [[CrossRef](#)]
41. Moussa, C.; Hebron, M.; Huang, X.; Ahn, J.; Rissman, R.A.; Aisen, P.S.; Turner, R.S. Resveratrol regulates neuro-inflammation and induces adaptive immunity in Alzheimer's disease. *J. Neuroinflamm.* **2017**, *14*, 1. [[CrossRef](#)]
42. Nazem, A.; Sankowski, R.; Bacher, M.; Al-Abed, Y. Rodent models of neuroinflammation for Alzheimer's disease. *J. Neuroinflamm.* **2015**, *12*, 74. [[CrossRef](#)] [[PubMed](#)]
43. Gillette-Guyonnet, S.; Nourhashemi, F.; Andrieu, S.; de Glizezinski, I.; Ousset, P.J.; Riviere, D.; Albarede, J.L.; Vellas, B. Weight loss in Alzheimer disease. *Am. J. Clin. Nutr.* **2000**, *71*, 637S–642S. [[CrossRef](#)] [[PubMed](#)]
44. Raji, C.A.; Lopez, O.L.; Kuller, L.H.; Carmichael, O.T.; Becker, J.T. Age, Alzheimer disease, and brain structure. *Neurology* **2009**, *73*, 1899–1905. [[CrossRef](#)] [[PubMed](#)]
45. Sepulveda, C.; Hernandez, B.; Burgos, C.F.; Fuentes, E.; Palomo, I.; Alarcon, M. The cAMP/PKA pathway inhibits beta-amyloid peptide release from human platelets. *Neuroscience* **2019**, *397*, 159–171. [[CrossRef](#)] [[PubMed](#)]

46. Szablewski, L. Glucose transporters in brain in health and in Alzheimer's disease. *J. Alzheimers Dis.* **2017**, *55*, 1307–1320. [[CrossRef](#)] [[PubMed](#)]
47. Mosconi, L. Glucose metabolism in normal aging and Alzheimer's disease: Methodological and physiological considerations for PET studies. *Clin. Transl. Imaging* **2013**, *1*. [[CrossRef](#)]
48. Resende, R.; Moreira, P.I.; Proenca, T.; Deshpande, A.; Busciglio, J.; Pereira, C.; Oliveira, C.R. Brain oxidative stress in a triple-transgenic mouse model of Alzheimer disease. *Free Radic. Biol. Med.* **2008**, *44*, 2051–2057. [[CrossRef](#)]
49. Nunomura, A.; Perry, G.; Aliev, G.; Hirai, K.; Takeda, A.; Balraj, E.K.; Jones, P.K.; Ghanbari, H.; Wataya, T.; Shimohama, S.; et al. Oxidative damage is the earliest event in Alzheimer disease. *J. Neuropathol. Exp. Neurol.* **2001**, *60*, 759–767. [[CrossRef](#)]
50. Sanchez-Martin, P.; Saito, T.; Komatsu, M. p62/SQSTM1: 'Jack of all trades' in health and cancer. *FEBS J.* **2019**, *286*, 8–23. [[CrossRef](#)]
51. Santos, R.X.; Correia, S.C.; Wang, X.; Perry, G.; Smith, M.A.; Moreira, P.I.; Zhu, X. A synergistic dysfunction of mitochondrial fission/fusion dynamics and mitophagy in Alzheimer's disease. *J. Alzheimers Dis.* **2010**, *20* (Suppl. 2), S401–S412. [[CrossRef](#)]
52. Xiong, H.; Zheng, C.; Wang, J.; Song, J.; Zhao, G.; Shen, H.; Deng, Y. The neuroprotection of liraglutide on Alzheimer-like learning and memory impairment by modulating the hyperphosphorylation of tau and neurofilament proteins and insulin signaling pathways in mice. *J. Alzh. Dis.* **2013**, *37*, 623–635. [[CrossRef](#)] [[PubMed](#)]
53. Yang, Y.; Zhang, J.; Ma, D.; Zhang, M.; Hu, S.; Shao, S.; Gong, C.X. Subcutaneous administration of liraglutide ameliorates Alzheimer-associated tau hyperphosphorylation in rats with type 2 diabetes. *J. Alzh. Dis.* **2013**, *37*, 637–648. [[CrossRef](#)] [[PubMed](#)]
54. Hansen, H.H.; Fabricius, K.; Barkholt, P.; Kongsbak-Wismann, P.; Schlumberger, C.; Jelsing, J.; Terwel, D.; Termont, A.; Pyke, C.; Knudsen, L.B.; et al. Long-term treatment with liraglutide, a glucagon-like peptide-1 (GLP-1) receptor agonist, has no effect on β -amyloid plaque load in two transgenic APP/PS1 mouse models of Alzheimer's disease. *PLoS ONE* **2016**, *11*, e0158205. [[CrossRef](#)] [[PubMed](#)]
55. Augustinack, J.C.; Schneider, A.; Mandelkow, E.M.; Hyman, B.T. Specific tau phosphorylation sites correlate with severity of neuronal cytopathology in Alzheimer's disease. *Acta Neuropathol.* **2002**, *103*, 26–35. [[CrossRef](#)] [[PubMed](#)]
56. Hoffmann, R.; Lee, V.M.Y.; Leight, S.; Varga, I.; Otvos, L., Jr. Unique Alzheimer's disease paired helical filament specific epitopes involve double phosphorylation at specific sites. *Biochemistry* **1997**, *36*, 8114–8124. [[CrossRef](#)]
57. Carvalho, C.; Cardoso, S.; Correia, S.C.; Santos, R.X.; Santos, M.S.; Baldeiras, I.; Oliveira, C.R.; Moreira, P.I. Metabolic alterations induced by sucrose intake and Alzheimer's disease promote similar brain mitochondrial abnormalities. *Diabetes* **2012**, *61*, 1234–1242. [[CrossRef](#)]
58. Belfiore, R.; Rodin, A.; Ferreira, E.; Velazquez, R.; Branca, C.; Caccamo, A.; Oddo, S. Temporal and regional progression of Alzheimer's disease-like pathology in 3xTg-AD mice. *Aging Cell* **2019**, *18*, e12873. [[CrossRef](#)]
59. Candeias, E.; Duarte, A.I.; Sebastiao, I.; Fernandes, M.A.; Placido, A.I.; Carvalho, C.; Correia, S.; Santos, R.X.; Seica, R.; Santos, M.S.; et al. Middle-aged diabetic females and males present distinct susceptibility to Alzheimer disease-like pathology. *Mol. Neurobiol.* **2017**, *54*, 6471–6489. [[CrossRef](#)]
60. Valencak, T.G.; Osterrieder, A.; Schulz, T.J. Sex matters: The effects of biological sex on adipose tissue biology and energy metabolism. *Redox Biol.* **2017**, *12*, 806–813. [[CrossRef](#)]
61. Goyal, M.S.; Blazey, T.M.; Su, Y.; Couture, L.E.; Durbin, T.J.; Bateman, R.J.; Benzinger, T.L.; Morris, J.C.; Raichle, M.E.; Vlassenko, A.G. Persistent metabolic youth in the aging female brain. *Proc. Natl. Acad. Sci. USA* **2019**, *116*, 3251–3255. [[CrossRef](#)]
62. Yan, H.; Yang, W.; Zhou, F.; Li, X.; Pan, Q.; Shen, Z.; Han, G.; Newell-Fugate, A.; Tian, Y.; Majeti, R.; et al. Estrogen improves insulin sensitivity and suppresses gluconeogenesis via the transcription factor Foxo1. *Diabetes* **2019**, *68*, 291–304. [[CrossRef](#)] [[PubMed](#)]
63. Haraguchi, S.; Sasahara, K.; Shikimi, H.; Honda, S.-i.; Harada, N.; Tsutsui, K. Estradiol promotes Purkinje dendritic growth, spinogenesis, and synaptogenesis during neonatal life by inducing the expression of BDNF. *Cerebellum* **2011**, *11*, 416–417. [[CrossRef](#)]

64. Dave, K.A.; Platel, J.-C.; Huang, F.; Tian, D.; Stambouliau-Platel, S.; Bordey, A. Prostaglandin E2 induces glutamate release from subventricular zone astrocytes. *Neuron Glia Biol.* **2010**, *6*, 201–207. [[CrossRef](#)] [[PubMed](#)]
65. Yang, L. Neuronal cAMP/PKA signaling and energy homeostasis. *Adv. Exp. Med. Biol.* **2018**, *1090*, 31–48. [[CrossRef](#)] [[PubMed](#)]
66. Gejl, M.; Lerche, S.; Egefjord, L.; Brock, B.; Moller, N.; Vang, K.; Rodell, A.B.; Bibby, B.M.; Holst, J.J.; Rungby, J.; et al. Glucagon-like peptide-1 (GLP-1) raises blood-brain glucose transfer capacity and hexokinase activity in human brain. *Front. Neuroenergetics* **2013**, *5*, 2. [[CrossRef](#)] [[PubMed](#)]
67. Gejl, M.; Egefjord, L.; Lerche, S.; Vang, K.; Bibby, B.M.; Holst, J.J.; Mengel, A.; Moller, N.; Rungby, J.; Brock, B.; et al. Glucagon-like peptide-1 decreases intracerebral glucose content by activating hexokinase and changing glucose clearance during hyperglycemia. *J. Cereb. Blood Flow Metab.* **2012**, *32*, 2146–2152. [[CrossRef](#)] [[PubMed](#)]
68. Cova, I.; Clerici, F.; Rossi, A.; Cucumo, V.; Ghiretti, R.; Maggiore, L.; Pomati, S.; Galimberti, D.; Scarpini, E.; Mariani, C.; et al. Weight loss predicts progression of mild cognitive impairment to Alzheimer's disease. *PLoS ONE* **2016**, *11*, e0151710. [[CrossRef](#)]
69. Duarte, A.I.; Sjogren, M.; Santos, M.S.; Oliveira, C.R.; Moreira, P.I.; Bjorkqvist, M. Dual therapy with liraglutide and ghrelin promotes brain and peripheral energy metabolism in the R6/2 mouse model of Huntington's disease. *Sci. Rep.* **2018**, *8*, 8961. [[CrossRef](#)]
70. Hansen, H.H.; Fabricius, K.; Barkholt, P.; Niehoff, M.L.; Morley, J.E.; Jelsing, J.; Pyke, C.; Knudsen, L.B.; Farr, S.A.; Vrang, N. The GLP-1 receptor agonist liraglutide improves memory function and increases hippocampal CA1 neuronal numbers in a senescence-accelerated mouse model of Alzheimer's disease. *J. Alzh. Dis.* **2015**, *46*, 877–888. [[CrossRef](#)]
71. Rollins, C.P.E.; Gallino, D.; Kong, V.; Ayranci, G.; Devenyi, G.A.; Germann, J.; Chakravarty, M.M. Contributions of a high-fat diet to Alzheimer's disease-related decline: A longitudinal behavioural and structural neuroimaging study in mouse models. *Neuroimage Clin.* **2018**, *21*, 101606. [[CrossRef](#)]
72. Cardoso, S.; Seica, R.; Moreira, P.I. Diabesity and brain energy metabolism: The case of Alzheimer's Disease. *Adv. Neurobiol.* **2017**, *19*, 117–150. [[CrossRef](#)] [[PubMed](#)]
73. Ott, A.; Stolk, R.P.; van Harskamp, F.; Pols, H.A.; Hofman, A.; Breteler, M.M. Diabetes mellitus and the risk of dementia: The Rotterdam Study. *Neurology* **1999**, *53*, 1937–1942. [[CrossRef](#)] [[PubMed](#)]
74. Leibson, C.L.; Rocca, W.A.; Hanson, V.A.; Cha, R.; Kokmen, E.; O'Brien, P.C.; Palumbo, P.J. The risk of dementia among persons with diabetes mellitus: A population-based cohort study. *Ann. N. Y. Acad. Sci.* **1997**, *826*, 422–427. [[CrossRef](#)] [[PubMed](#)]
75. Morris, J.K.; John, C.S.; Wilkins, H.M.; Wang, X.; Weidling, I.; Thyfault, J.P.; Vidoni, E.D.; Swerdlow, R.H.; Burns, J.M. Alzheimer's disease subjects exhibit impaired systemic glucose metabolism following a mixed meal. *Alzh. Dement.* **2018**, *14*, 1159–1160. [[CrossRef](#)]
76. Kilander, L.; Boberg, M.; Lithell, H. Peripheral glucose metabolism and insulin sensitivity in Alzheimer's disease. *Acta Neurol. Scand.* **1993**, *87*, 294–298. [[CrossRef](#)] [[PubMed](#)]
77. Femminella, G.D.; Frangou, E.; Love, S.B.; Busza, G.; Holmes, C.; Ritchie, C.; Lawrence, R.; McFarlane, B.; Tadros, G.; Ridha, B.H.; et al. Evaluating the effects of the novel GLP-1 analogue liraglutide in Alzheimer's disease: Study protocol for a randomised controlled trial (ELAD study). *Trials* **2019**, *20*, 191. [[CrossRef](#)] [[PubMed](#)]
78. Patching, S.G. Glucose transporters at the blood-brain barrier: Function, regulation and gateways for drug delivery. *Mol. Neurobiol.* **2017**, *54*, 1046–1077. [[CrossRef](#)]
79. Liu, Y.; Liu, F.; Grundke-Iqbal, I.; Iqbal, K.; Gong, C.X. Deficient brain insulin signalling pathway in Alzheimer's disease and diabetes. *J. Pathol.* **2011**, *225*, 54–62. [[CrossRef](#)]
80. Nordberg, A.; Rinne, J.O.; Kadir, A.; Långström, B. The use of PET in Alzheimer disease. *Nat. Rev. Neurol.* **2010**, *6*, 78–87. [[CrossRef](#)]
81. Liu, Y.; Liu, F.; Grundke-Iqbal, I.; Iqbal, K.; Gong, C.X. Brain glucose transporters, O-GlcNAcylation and phosphorylation of tau in diabetes and Alzheimer's disease. *J. Neurochem.* **2009**, *111*, 242–249. [[CrossRef](#)]
82. Liu, Y.; Liu, F.; Iqbal, K.; Grundke-Iqbal, I.; Gong, C.X. Decreased glucose transporters correlate to abnormal hyperphosphorylation of tau in Alzheimer disease. *FEBS Lett.* **2008**, *582*, 359–364. [[CrossRef](#)] [[PubMed](#)]

83. Mosconi, L.; Tsui, W.H.; Herholz, K.; Pupi, A.; Drzezga, A.; Lucignani, G.; Reiman, E.M.; Holthoff, V.; Kalbe, E.; Sorbi, S.; et al. Multicenter standardized 18F-FDG PET diagnosis of mild cognitive impairment, Alzheimer's disease, and other dementias. *J. Nucl. Med.* **2008**, *49*, 390–398. [[CrossRef](#)] [[PubMed](#)]
84. Wiciński, M.; Szadujkis-Szadurska, K.; Węclewicz, M.M.; Malinowski, B.; Matusiak, G.; Walczak, M.; Wódkiewicz, E.; Grzešek, G.; Pawlak-Osińska, K. The role of Rho-kinase and calcium ions in constriction triggered by ET-1. *Microvasc. Res.* **2018**, *119*, 84–90. [[CrossRef](#)]
85. Wiciński, M.; Socha, M.; Walczak, M.; Wódkiewicz, E.; Malinowski, B.; Rewerski, S.; Górski, K.; Pawlak-Osińska, K. Beneficial effects of resveratrol administration—Focus on potential biochemical mechanisms in cardiovascular conditions. *Nutrients* **2018**, *10*, 1813. [[CrossRef](#)]
86. Gejl, M.; Brock, B.; Egefjord, L.; Vang, K.; Rungby, J.; Gjedde, A. Blood-Brain glucose transfer in Alzheimer's disease: Effect of GLP-1 analog treatment. *Sci. Rep.* **2017**, *7*, 17490. [[CrossRef](#)] [[PubMed](#)]
87. Winkler, E.A.; Nishida, Y.; Sagare, A.P.; Rege, S.V.; Bell, R.D.; Perlmutter, D.; Sengillo, J.D.; Hillman, S.; Kong, P.; Nelson, A.R.; et al. GLUT1 reductions exacerbate Alzheimer's disease vasculo-neuronal dysfunction and degeneration. *Nat. Neurosci.* **2015**, *18*, 521–530. [[CrossRef](#)]
88. García-Cáceres, C.; Quarta, C.; Varela, L.; Gao, Y.; Gruber, T.; Legutko, B.; Jastroch, M.; Johansson, P.; Ninkovic, J.; Yi, C.-X.; et al. Astrocytic insulin signaling couples brain glucose uptake with nutrient availability. *Cell* **2016**, *166*, 867–880. [[CrossRef](#)]
89. Hernandez-Garzón, E.; Fernandez, A.M.; Perez-Alvarez, A.; Genis, L.; Bascuñana, P.; de la Rosa, R.F.; Delgado, M.; Pozo, M.A.; Moreno, E.; McCormick, P.J.; et al. The insulin-like growth factor I receptor regulates glucose transport by astrocytes. *Glia* **2016**, *64*, 1962–1971. [[CrossRef](#)]
90. Jais, A.; Solas, M.; Backes, H.; Chaurasia, B.; Kleinridders, A.; Theurich, S.; Mauer, J.; Steculorum, S.M.; Hampel, B.; Goldau, J.; et al. Myeloid-cell-derived VEGF maintains brain glucose uptake and limits cognitive impairment in obesity. *Cell* **2016**, *165*, 882–895. [[CrossRef](#)]
91. Xiao-Yun, X.; Zhao-Hui, M.; Ke, C.; Hong-Hui, H.; Yan-Hong, X. Glucagon-like peptide-1 improves proliferation and differentiation of endothelial progenitor cells via upregulating VEGF generation. *Med. Sci. Monit.* **2011**, *17*, BR35–BR41. [[CrossRef](#)]
92. Madadi, G.; Dalvi, P.S.; Belsham, D.D. Regulation of brain insulin mRNA by glucose and glucagon-like peptide 1. *Biochem. Biophys. Res. Commun.* **2008**, *376*, 694–699. [[CrossRef](#)] [[PubMed](#)]
93. Gejl, M.; Gjedde, A.; Egefjord, L.; Møller, A.; Hansen, S.B.; Vang, K.; Rodell, A.; Brændgaard, H.; Gottrup, H.; Schacht, A.; et al. In Alzheimer's disease, 6-month treatment with GLP-1 analog prevents decline of brain glucose metabolism: Randomized, placebo-controlled, double-blind clinical trial. *Front. Aging Neurosci.* **2016**, *8*, 108. [[CrossRef](#)] [[PubMed](#)]
94. Lai, K.S.P.; Liu, C.S.; Rau, A.; Lanctot, K.L.; Kohler, C.A.; Pakosh, M.; Carvalho, A.F.; Herrmann, N. Peripheral inflammatory markers in Alzheimer's disease: A systematic review and meta-analysis of 175 studies. *J. Neurol. Neurosurg. Psychiatry* **2017**, *88*, 876–882. [[CrossRef](#)] [[PubMed](#)]
95. Ramamoorthy, M.; Sykora, P.; Scheibye-Knudsen, M.; Dunn, C.; Kasmer, C.; Zhang, Y.; Becker, K.G.; Croteau, D.L.; Bohr, V.A. Sporadic Alzheimer disease fibroblasts display an oxidative stress phenotype. *Free Radic. Biol. Med.* **2012**, *53*, 1371–1380. [[CrossRef](#)] [[PubMed](#)]
96. Swardfager, W.; Lanctot, K.; Rothenburg, L.; Wong, A.; Cappell, J.; Herrmann, N. A meta-analysis of cytokines in Alzheimer's disease. *Biol. Psychiatry* **2010**, *68*, 930–941. [[CrossRef](#)]
97. Moreira, P.I.; Harris, P.L.; Zhu, X.; Santos, M.S.; Oliveira, C.R.; Smith, M.A.; Perry, G. Lipoic acid and N-acetyl cysteine decrease mitochondrial-related oxidative stress in Alzheimer disease patient fibroblasts. *J. Alzheimers Dis.* **2007**, *12*, 195–206. [[CrossRef](#)]
98. Yao, J.; Irwin, R.W.; Zhao, L.; Nilsen, J.; Hamilton, R.T.; Brinton, R.D. Mitochondrial bioenergetic deficit precedes Alzheimer's pathology in female mouse model of Alzheimer's disease. *Proc. Natl. Acad. Sci. USA* **2009**, *106*, 14670–14675. [[CrossRef](#)]
99. Cenini, G.; Sultana, R.; Memo, M.; Butterfield, D.A. Effects of oxidative and nitrosative stress in brain on p53 proapoptotic protein in amnesic mild cognitive impairment and Alzheimer disease. *Free Radic. Biol. Med.* **2008**, *45*, 81–85. [[CrossRef](#)]
100. Calabrese, V.; Sultana, R.; Scapagnini, G.; Guagliano, E.; Sapienza, M.; Bella, R.; Kanski, J.; Pennisi, G.; Mancuso, C.; Stella, A.M.; et al. Nitrosative stress, cellular stress response, and thiol homeostasis in patients with Alzheimer's disease. *Antioxid. Redox Signal.* **2006**, *8*, 1975–1986. [[CrossRef](#)]

101. Baker, S.K.; Chen, Z.L.; Norris, E.H.; Revenko, A.S.; MacLeod, A.R.; Strickland, S. Blood-derived plasminogen drives brain inflammation and plaque deposition in a mouse model of Alzheimer's disease. *Proc. Natl. Acad. Sci. USA* **2018**, *115*, E9687–E9696. [[CrossRef](#)]
102. Choi, S.; Won, J.S.; Carroll, S.L.; Annamalai, B.; Singh, I.; Singh, A.K. Pathology of nNOS-expressing GABAergic neurons in mouse model of Alzheimer's disease. *Neuroscience* **2018**, *384*, 41–53. [[CrossRef](#)]
103. Placido, A.I.; Oliveira, C.R.; Moreira, P.I.; Pereira, C.M. Enhanced amyloidogenic processing of amyloid precursor protein and cell death under prolonged endoplasmic reticulum stress in brain endothelial cells. *Mol. Neurobiol.* **2015**, *51*, 571–590. [[CrossRef](#)] [[PubMed](#)]
104. O'Connor, T.; Sadleir, K.R.; Maus, E.; Velliquette, R.A.; Zhao, J.; Cole, S.L.; Eimer, W.A.; Hitt, B.; Bembinster, L.A.; Lammich, S.; et al. Phosphorylation of the translation initiation factor eIF2 α increases BACE1 levels and promotes amyloidogenesis. *Neuron* **2008**, *60*, 988–1009. [[CrossRef](#)] [[PubMed](#)]
105. Herrup, K. Reimagining Alzheimer's disease—An age-based hypothesis. *J. Neurosci.* **2010**, *30*, 16755–16762. [[CrossRef](#)] [[PubMed](#)]
106. Perry, V.H.; Nicoll, J.A.; Holmes, C. Microglia in neurodegenerative disease. *Nat. Rev. Neurol.* **2010**, *6*, 193–201. [[CrossRef](#)] [[PubMed](#)]
107. Forlenza, O.V.; Diniz, B.S.; Talib, L.L.; Mendonca, V.A.; Ojopi, E.B.; Gattaz, W.F.; Teixeira, A.L. Increased serum IL-1 β level in Alzheimer's disease and mild cognitive impairment. *Dement. Geriatr. Cogn. Disord.* **2009**, *28*, 507–512. [[CrossRef](#)]
108. Shaftel, S.S.; Griffin, W.S.; O'Banion, M.K. The role of interleukin-1 in neuroinflammation and Alzheimer disease: An evolving perspective. *J. Neuroinflamm.* **2008**, *5*, 7. [[CrossRef](#)]
109. Chakrabarty, P.; Li, A.; Ceballos-Diaz, C.; Eddy, J.A.; Funk, C.C.; Moore, B.; DiNunno, N.; Rosario, A.M.; Cruz, P.E.; Verbeeck, C.; et al. IL-10 alters immunoproteostasis in APP mice, increasing plaque burden and worsening cognitive behaviour. *Neuron* **2015**, *85*, 519–533. [[CrossRef](#)]
110. Guillot-Sestier, M.V.; Doty, K.R.; Gate, D.; Rodriguez, J., Jr.; Leung, B.P.; Rezai-Zadeh, K.; Town, T. IL10 deficiency rebalances innate immunity to mitigate Alzheimer-like pathology. *Neuron* **2015**, *85*, 534–548. [[CrossRef](#)]
111. He, W.; Tian, X.; Lv, M.; Wang, H. Liraglutide protects neurite outgrowth of cortical neurons under oxidative stress through activating the Wnt pathway. *J. Stroke Cerebrovasc. Dis.* **2018**, *27*, 2696–2702. [[CrossRef](#)]
112. Wiciński, M.; Socha, M.; Malinowski, B.; Wódkiewicz, E.; Walczak, M.; Górski, K.; Słupski, M.; Pawlak-Osińska, K. Liraglutide and its neuroprotective properties—Focus on possible biochemical mechanisms in Alzheimer's disease and cerebral ischemic events. *Int. J. Mol. Sci.* **2019**, *20*, 1050. [[CrossRef](#)] [[PubMed](#)]
113. Shiraki, A.; Oyama, J.i.; Komoda, H.; Asaka, M.; Komatsu, A.; Sakuma, M.; Kodama, K.; Sakamoto, Y.; Kotooka, N.; Hirase, T.; et al. The glucagon-like peptide 1 analog liraglutide reduces TNF- α -induced oxidative stress and inflammation in endothelial cells. *Atherosclerosis* **2012**, *221*, 375–382. [[CrossRef](#)] [[PubMed](#)]
114. Han, L.; Hölscher, C.; Xue, G.F.; Li, G.; Li, D. A novel dual-glucagon-like peptide-1 and glucose-dependent insulinotropic polypeptide receptor agonist is neuroprotective in transient focal cerebral ischemia in the rat. *Neuroreport* **2016**, *27*, 23–32. [[CrossRef](#)] [[PubMed](#)]
115. Zhu, H.; Zhang, Y.; Shi, Z.; Lu, D.; Li, T.; Ding, Y.; Ruan, Y.; Xu, A. The neuroprotection of liraglutide against ischaemia-induced apoptosis through the activation of the PI3K/AKT and MAPK pathways. *Sci. Rep.* **2016**, *6*, 26859. [[CrossRef](#)]
116. Zhang, Y.; Hu, S.-Y.; Yin, T.; Tian, F.; Wang, S.; Zhang, Y.; Chen, Y.D. [Liraglutide Promotes Proliferation and Migration of Cardiac Microvascular Endothelial Cells Through PI3K/Akt and MAPK/ERK Signaling Pathways]. *J. South. Med. Univ.* **2015**, *35*, 1221–1226.
117. Zhou, H.; Li, D.; Shi, C.; Xin, T.; Yang, J.; Zhou, Y.; Hu, S.; Tian, F.; Wang, J.; Chen, Y. Effects of exendin-4 on bone marrow mesenchymal stem cell proliferation, migration and apoptosis in vitro. *Sci. Rep.* **2015**, *5*, 12898. [[CrossRef](#)]
118. Briyal, S.; Shah, S.; Gulati, A. Neuroprotective and anti-apoptotic effects of liraglutide in the rat brain following focal cerebral ischemia. *Neuroscience* **2014**, *281*, 269–281. [[CrossRef](#)]
119. Hamamoto, S.; Kanda, Y.; Shimoda, M.; Tatsumi, F.; Kohara, K.; Tawaramoto, K.; Hashiramoto, M.; Kaku, K. Vildagliptin preserves the mass and function of pancreatic β cells via the developmental regulation and suppression of oxidative and endoplasmic reticulum stress in a mouse model of diabetes. *Diabetes Obes. Metab.* **2013**, *15*, 153–163. [[CrossRef](#)]

120. Sato, K.; Kameda, M.; Yasuhara, T.; Agari, T.; Baba, T.; Wang, F.; Shinko, A.; Wakamori, T.; Toyoshima, A.; Takeuchi, H.; et al. Neuroprotective effects of liraglutide for stroke model of rats. *Int. J. Mol. Sci.* **2013**, *14*, 21513–21524. [[CrossRef](#)]
121. Talbot, K.; Wang, H.-Y.; Kazi, H.; Han, L.-Y.; Bakshi, K.P.; Stucky, A.; Fuino, R.L.; Kawaguchi, K.R.; Samoyedny, A.J.; Wilson, R.S.; et al. Demonstrated brain insulin resistance in Alzheimer's disease patients is associated with IGF-1 resistance, IRS-1 dysregulation, and cognitive decline. *J. Clin. Investig.* **2012**, *122*, 1316–1338. [[CrossRef](#)]
122. Jalewa, J.; Sharma, M.K.; Hölscher, C. Novel incretin analogues improve autophagy and protect from mitochondrial stress induced by rotenone in SH-SY5Y cells. *J. Neurochem.* **2016**, *139*, 55–67. [[CrossRef](#)] [[PubMed](#)]
123. Wang, R.-F.; Xue, G.-F.; Hölscher, C.; Tian, M.-J.; Feng, P.; Zheng, J.-Y.; Li, D.-F. Post-treatment with the GLP-1 analogue liraglutide alleviate chronic inflammation and mitochondrial stress induced by Status epilepticus. *Epilepsy Res.* **2018**, *142*, 45–52. [[CrossRef](#)]
124. Ji, C.; Xue, G.-F.; Lijun, C.; Feng, P.; Li, D.; Li, L.; Li, G.; Hölscher, C. A novel dual GLP-1 and GIP receptor agonist is neuroprotective in the MPTP mouse model of Parkinson's disease by increasing expression of BDNF. *Brain Res.* **2016**, *1634*, 1–11. [[CrossRef](#)] [[PubMed](#)]
125. Li, P.C.; Liu, L.F.; Jou, M.J.; Wang, H.K. The GLP-1 receptor agonists exendin-4 and liraglutide alleviate oxidative stress and cognitive and micturition deficits induced by middle cerebral artery occlusion in diabetic mice. *BMC Neurosci.* **2016**, *17*, 37. [[CrossRef](#)] [[PubMed](#)]
126. Zhang, H.; Liu, Y.; Guan, S.; Qu, D.; Wang, L.; Wang, X.; Li, X.; Zhou, S.; Zhou, Y.; Wang, N.; et al. An orally active allosteric GLP-1 receptor agonist is neuroprotective in cellular and rodent models of stroke. *PLoS ONE* **2016**, *11*, e0148827. [[CrossRef](#)] [[PubMed](#)]
127. Sharma, M.K.; Jalewa, J.; Hölscher, C. Neuroprotective and anti-apoptotic effects of liraglutide on SH-SY5Y cells exposed to methylglyoxal stress. *J. Neurochem.* **2014**, *128*, 459–471. [[CrossRef](#)]
128. Velmurugan, K.; Balamurugan, A.N.; Loganathan, G.; Ahmad, A.; Hering, B.J.; Pugazhenth, S. Antiapoptotic actions of exendin-4 against hypoxia and cytokines are augmented by CREB. *Endocrinology* **2012**, *153*, 1116–1128. [[CrossRef](#)]
129. Lozano, G.M.; Bejarano, I.; Espino, J.; González, D.; Ortiz, A.; García, J.F.; Rodríguez, A.B.; Pariente, J.A. Relationship between caspase activity and apoptotic markers in human sperm in response to hydrogen peroxide and progesterone. *J. Reprod. Dev.* **2009**, *55*, 615–621. [[CrossRef](#)]
130. He, W.; Wang, H.; Zhao, C.; Tian, X.; Li, L.; Wang, H. Role of liraglutide in brain repair promotion through Sirt1-mediated mitochondrial improvement in stroke. *J. Cell. Physiol.* **2020**, *235*, 2986–3001. [[CrossRef](#)]
131. Tong, W.; Ju, L.; Qiu, M.; Xie, Q.; Chen, Y.; Shen, W.; Sun, W.; Wang, W.; Tian, J. Liraglutide ameliorates non-alcoholic fatty liver disease by enhancing mitochondrial architecture and promoting autophagy through the SIRT1/SIRT3-FOXO3a pathway. *Hepatol. Res.* **2016**, *46*, 933–943. [[CrossRef](#)]
132. Deng, C.; Cao, J.; Han, J.; Li, J.; Li, Z.; Shi, N.; He, J. Liraglutide activates the Nrf2/HO-1 antioxidant pathway and protects brain nerve cells against cerebral ischemia in diabetic rats. *Comput. Intell. Neurosci.* **2018**, *2018*, 3094504. [[CrossRef](#)] [[PubMed](#)]
133. Bigl, M.; Bruckner, M.K.; Arendt, T.; Bigl, V.; Eschrich, K. Activities of key glycolytic enzymes in the brains of patients with Alzheimer's disease. *J. Neural. Transm.* **1999**, *106*, 499–511. [[CrossRef](#)] [[PubMed](#)]
134. Ansari, M.A.; Scheff, S.W. Oxidative stress in the progression of Alzheimer disease in the frontal cortex. *J. Neuropathol. Exp. Neurol.* **2010**, *69*, 155–167. [[CrossRef](#)] [[PubMed](#)]
135. Dai, Y.; Mehta, J.L.; Chen, M. Glucagon-like peptide-1 receptor agonist liraglutide inhibits endothelin-1 in endothelial cell by repressing nuclear factor-kappa B activation. *Cardiovasc. Drugs Ther.* **2013**, *27*, 371–380. [[CrossRef](#)] [[PubMed](#)]
136. McClean, P.L.; Hölscher, C. Liraglutide can reverse memory impairment, synaptic loss and reduce plaque load in aged APP/PS1 mice, a model of Alzheimer's disease. *Neuropharmacology* **2014**, *76 Pt A*, 57–67. [[CrossRef](#)]
137. Parthasarathy, V.; Hölscher, C. The type 2 diabetes drug liraglutide reduces chronic inflammation induced by irradiation in the mouse brain. *Eur. J. Pharmacol.* **2013**, *700*, 42–50. [[CrossRef](#)]
138. Barreto-Vianna, A.R.C.; Aguila, M.B.; Mandarin-de-Lacerda, C.A. Beneficial effects of liraglutide (GLP1 analog) in the hippocampal inflammation. *Metab. Brain Dis.* **2017**, *32*, 1735–1745. [[CrossRef](#)]

139. Gao, H.; Zeng, Z.; Zhang, H.; Zhou, X.; Guan, L.; Deng, W.; Xu, L. The Glucagon-Like Peptide-1 analogue liraglutide inhibits oxidative stress and inflammatory response in the liver of rats with diet-induced non-alcoholic fatty liver disease. *Biol. Pharm. Bull.* **2015**, *38*, 694–702. [[CrossRef](#)]
140. Wu, L.K.; Liu, Y.C.; Shi, L.L.; Lu, K.D. Glucagon-like peptide-1 receptor agonists inhibit hepatic stellate cell activation by blocking the p38 MAPK signaling pathway. *Genet. Mol. Res.* **2015**, *14*, 19087–19093. [[CrossRef](#)]
141. Tian, Y.; Huang, Z.; Wang, Z.; Yin, C.; Zhou, L.; Zhang, L.; Huang, K.; Zhou, H.; Jiang, X.; Li, J.; et al. Identification of novel molecular markers for prognosis estimation of acute myeloid leukemia: Over-expression of PDCD7, FIS1 and Ang2 may indicate poor prognosis in pretreatment patients with acute myeloid leukemia. *PLoS ONE* **2014**, *9*, e84150. [[CrossRef](#)]
142. Alavi, M.V.; Fuhrmann, N. Dominant optic atrophy, OPA1, and mitochondrial quality control: Understanding mitochondrial network dynamics. *Mol. Neurodegener.* **2013**, *8*, 32. [[CrossRef](#)] [[PubMed](#)]
143. Palmer, C.S.; Elgass, K.D.; Parton, R.G.; Osellame, L.D.; Stojanovski, D.; Ryan, M.T. Adaptor proteins MiD49 and MiD51 can act independently of Mff and Fis1 in Drp1 recruitment and are specific for mitochondrial fission. *J. Biol. Chem.* **2013**, *288*, 27584–27593. [[CrossRef](#)] [[PubMed](#)]
144. Olichon, A.; Baricault, L.; Gas, N.; Guillou, E.; Valette, A.; Belenguer, P.; Lenaers, G. Loss of OPA1 perturbs the mitochondrial inner membrane structure and integrity, leading to cytochrome c release and apoptosis. *J. Biol. Chem.* **2003**, *278*, 7743–7746. [[CrossRef](#)] [[PubMed](#)]
145. Elachouri, G.; Vidoni, S.; Zanna, C.; Pattyn, A.; Boukhaddaoui, H.; Gaget, K.; Yu-Wai-Man, P.; Gasparre, G.; Sarzi, E.; Delettre, C.; et al. OPA1 links human mitochondrial genome maintenance to mtDNA replication and distribution. *Genome Res.* **2011**, *21*, 12–20. [[CrossRef](#)] [[PubMed](#)]
146. Amati-Bonneau, P.; Valentino, M.L.; Reynier, P.; Gallardo, M.E.; Bornstein, B.; Boissiere, A.; Campos, Y.; Rivera, H.; de la Aleja, J.G.; Carroccia, R.; et al. OPA1 mutations induce mitochondrial DNA instability and optic atrophy ‘plus’ phenotypes. *Brain* **2008**, *131*, 338–351. [[CrossRef](#)] [[PubMed](#)]
147. Hudson, G.; Amati-Bonneau, P.; Blakely, E.L.; Stewart, J.D.; He, L.; Schaefer, A.M.; Griffiths, P.G.; Ahlqvist, K.; Suomalainen, A.; Reynier, P.; et al. Mutation of OPA1 causes dominant optic atrophy with external ophthalmoplegia, ataxia, deafness and multiple mitochondrial DNA deletions: A novel disorder of mtDNA maintenance. *Brain* **2008**, *131*, 329–337. [[CrossRef](#)] [[PubMed](#)]
148. Lees, J.P.; Manlandro, C.M.; Picton, L.K.; Tan, A.Z.; Casares, S.; Flanagan, J.M.; Fleming, K.G.; Hill, R.B. A designed point mutant in Fis1 disrupts dimerization and mitochondrial fission. *J. Mol. Biol.* **2012**, *423*, 143–158. [[CrossRef](#)]
149. Li, H.; Cao, L.; Ren, Y.; Jiang, Y.; Xie, W.; Li, D. GLP-1 receptor regulates cell growth through regulating IDE expression level in A β 1-42-treated PC12 cells. *Biosci. Rep.* **2018**, *38*, BSR20171284. [[CrossRef](#)]
150. Li, H.; Yang, S.; Wu, J.; Ji, L.; Zhu, L.; Cao, L.; Huang, J.; Jiang, Q.; Wei, J.; Liu, M.; et al. AMP/PKA signaling pathway contributes to neuronal apoptosis via regulating IDE expression in a mixed model of type 2 diabetes and Alzheimer’s disease. *J. Cell. Biochem.* **2018**, *119*, 1616–1626. [[CrossRef](#)]
151. Costa, R.; Ferreira-da-Silva, F.; Saraiva, M.J.; Cardoso, I. Transthyretin protects against A-beta peptide toxicity by proteolytic cleavage of the peptide: A mechanism sensitive to the Kunitz protease inhibitor. *PLoS ONE* **2008**, *3*, e2899. [[CrossRef](#)]
152. Costa, R.; Gonçalves, A.; Saraiva, M.J.; Cardoso, I. Transthyretin binding to A-Beta peptide—impact on A-Beta fibrillogenesis and toxicity. *FEBS Lett.* **2008**, *582*, 936–942. [[CrossRef](#)] [[PubMed](#)]
153. Carro, E.; Torres-Aleman, I. Serum insulin-like growth factor I in brain function. *Keio J. Med.* **2006**, *55*, 59–63. [[CrossRef](#)] [[PubMed](#)]
154. Carro, E.; Trejo, J.L.; Gerber, A.; Loetscher, H.; Torrado, J.; Metzger, F.; Torres-Aleman, I. Therapeutic actions of insulin-like growth factor I on APP/PS2 mice with severe brain amyloidosis. *Neurobiol. Aging* **2006**, *27*, 1250–1257. [[CrossRef](#)] [[PubMed](#)]
155. Padurariu, M.; Ciobica, A.; Mavroudis, I.; Fotiou, D.; Baloyannis, S. Hippocampal neuronal loss in the CA1 and CA3 areas of Alzheimer’s disease patients. *Psychiatr. Danub.* **2012**, *24*, 152–158. [[PubMed](#)]
156. Rissman, R.A.; Poon, W.W.; Blurton-Jones, M.; Oddo, S.; Torp, R.; Vitek, M.P.; LaFerla, F.M.; Rohn, T.T.; Cotman, C.W. Caspase-cleavage of tau is an early event in Alzheimer disease tangle pathology. *J. Clin. Invest.* **2004**, *114*, 121–130. [[CrossRef](#)]
157. Ayala-Grosso, C.; Ng, G.; Roy, S.; Robertson, G.S. Caspase-cleaved amyloid precursor protein in Alzheimer’s disease. *Brain Pathol.* **2002**, *12*, 430–441. [[CrossRef](#)]

158. Koshal, P.; Kumar, P. Neurochemical modulation involved in the beneficial effect of liraglutide, GLP-1 agonist on PTZ kindling epilepsy-induced comorbidities in mice. *Mol. Cell. Biochem.* **2016**, *415*, 77–87. [[CrossRef](#)]
159. Koshal, P.; Kumar, P. Effect of Liraglutide on Corneal Kindling Epilepsy Induced Depression and Cognitive Impairment in Mice. *Neurochem. Res.* **2016**, *41*, 1741–1750. [[CrossRef](#)]
160. McClean, P.L.; Gault, V.A.; Harriott, P.; Hölscher, C. Glucagon-like peptide-1 analogues enhance synaptic plasticity in the brain: A link between diabetes and Alzheimer's disease. *Eur. J. Pharmacol.* **2010**, *630*, 158–162. [[CrossRef](#)]
161. Babateen, O.; Korol, S.V.; Jin, Z.; Bhandage, A.K.; Ahemaiti, A.; Birnir, B. Liraglutide modulates GABAergic signaling in rat hippocampal CA3 pyramidal neurons predominantly by presynaptic mechanism. *BMC Pharmacol. Toxicol.* **2017**, *18*, 83. [[CrossRef](#)]
162. Gupta, G.; Dahiya, R.; Dua, K.; Chellappan, D.K.; Tiwari, J.; Sharma, G.N.; Singh, S.K.; Mishra, A.; Sharma, R.K.; Agrawal, M. Anticonvulsant effect of liraglutide, GLP-1 agonist by averting a change in GABA and brain glutathione level on picrotoxin-induced seizures. *EXCLI J.* **2017**, *16*, 752–754. [[CrossRef](#)] [[PubMed](#)]
163. Gilman, C.P.; Perry, T.; Furukawa, K.; Grieg, N.H.; Egan, J.M.; Mattson, M.P. Glucagon-like peptide 1 modulates calcium responses to glutamate and membrane depolarization in hippocampal neurons. *J. Neurochem.* **2003**, *87*, 1137–1144. [[CrossRef](#)] [[PubMed](#)]
164. Li, M.; Li, S.; Li, Y. Liraglutide promotes cortical neurite outgrowth via the MEK-ERK pathway. *Cell. Mol. Neurobiol.* **2015**, *35*, 987–993. [[CrossRef](#)] [[PubMed](#)]
165. Ma, X.; Lin, W.; Lin, Z.; Hao, M.; Gao, X.; Zhang, Y.; Kuang, H. Liraglutide alleviates H₂O₂-induced retinal ganglion cells injury by inhibiting autophagy through mitochondrial pathways. *Peptides* **2017**, *92*, 1–8. [[CrossRef](#)]
166. Meier, J.J. GLP-1 receptor agonists for individualized treatment of type 2 diabetes mellitus. *Nat. Rev. Endocrinol.* **2012**, *8*, 728–742. [[CrossRef](#)]
167. Wiciński, M.; Malinowski, B.; Węclewicz, M.M.; Grześk, E.; Grześk, G. Anti-atherogenic properties of resveratrol: 4-week resveratrol administration associated with serum concentrations of SIRT1, adiponectin, S100A8/A9 and VSMCs contractility in a rat model. *Exp. Ther. Med.* **2017**, *13*, 2071–2078. [[CrossRef](#)]
168. Parthasarathy, V.; Hölscher, C. Chronic treatment with the GLP1 analogue liraglutide increases cell proliferation and differentiation into neurons in an AD mouse model. *PLoS ONE* **2013**, *8*, e58784. [[CrossRef](#)]
169. Salcedo, I.; Tweedie, D.; Li, Y.; Greig, N.H. Neuroprotective and neurotrophic actions of glucagon-like peptide-1: An emerging opportunity to treat neurodegenerative and cerebrovascular disorders. *Br. J. Pharmacol.* **2012**, *166*, 1586–1599. [[CrossRef](#)]
170. Dong, W.; Miao, Y.; Chen, A.; Cheng, M.; Ye, X.; Song, F.; Zheng, G. Delayed administration of the GLP-1 receptor agonist liraglutide improves metabolic and functional recovery after cerebral ischemia in rats. *Neurosci. Lett.* **2017**, *641*, 1–7. [[CrossRef](#)]
171. Briyal, S.; Gulati, K.; Gulati, A. Repeated administration of exendin-4 reduces focal cerebral ischemia-induced infarction in rats. *Brain Res.* **2012**, *1427*, 23–34. [[CrossRef](#)]
172. Schaar, K.L.; Brenneman, M.M.; Savitz, S.I. Functional assessments in the rodent stroke model. *Exp. Transl. Stroke Med.* **2010**, *2*, 13. [[CrossRef](#)]
173. Gentilella, R.; Pechtner, V.; Corcos, A.; Consoli, A. Glucagon-like peptide-1 receptor agonists in type 2 diabetes treatment: Are they all the same? *Diabetes Metab. Res. Rev.* **2019**, *35*, e3070. [[CrossRef](#)] [[PubMed](#)]
174. Lin, C.H.; Hsieh, S.H.; Sun, J.H.; Tsai, J.S.; Huang, Y.Y. Glucose variability and β -cell response by GLP-1 analogue added-on CSII for patients with poorly controlled type 2 diabetes. *Sci. Rep.* **2015**, *5*, 16968. [[CrossRef](#)]
175. Salehi, M.; Aulinger, B.; Prigeon, R.L.; D'Alessio, D.A. Effect of endogenous GLP-1 on insulin secretion in type 2 diabetes. *Diabetes* **2010**, *59*, 1330–1337. [[CrossRef](#)] [[PubMed](#)]
176. Onoviran, O.F.; Li, D.; Toombs Smith, S.; Raji, M.A. Effects of glucagon-like peptide 1 receptor agonists on comorbidities in older patients with diabetes mellitus. *Ther. Adv. Chronic Dis.* **2019**, *10*. [[CrossRef](#)] [[PubMed](#)]
177. Harkavyi, A.; Abuirmeileh, A.; Lever, R.; Kingsbury, A.E.; Biggs, C.S.; Whitton, P.S. Glucagon-like peptide 1 receptor stimulation reverses key deficits in distinct rodent models of Parkinson's disease. *J. Neuroinflamm.* **2008**, *5*, 19. [[CrossRef](#)]
178. Armstrong, M.J.; Hull, D.; Guo, K.; Barton, D.; Hazlehurst, J.M.; Gathercole, L.L.; Nasiri, M.; Yu, J.; Stephen, C.; Gough, S.C.; et al. Glucagon-like peptide 1 decreases lipotoxicity in non-alcoholic steatohepatitis. *J. Hepatol.* **2016**, *64*, 399–408. [[CrossRef](#)]

179. Blackman, A.; Foster, G.D.; Zammit, G.; Rosenberg, R.; Aronne, L.; Wadden, T.; Claudius, B.; Jensen, C.B.; Mignot, E. Effect of liraglutide 3.0 mg in individuals with obesity and moderate or severe obstructive sleep apnea: The SCALE Sleep Apnea randomized clinical trial. *Int. J. Obes.* **2016**, *40*, 1310–1319. [[CrossRef](#)]
180. Simó, R.; Guerci, B.; Schernthaner, G.; Gallwitz, B.; Rosas-Guzmán, J.; Dotta, F.; Festa, A.; Zhou, M.; Kiljański, J. Long-term changes in cardiovascular risk markers during administration of exenatide twice daily or glimepiride: Results from the European exenatide study. *Cardiovasc. Diabetol.* **2015**, *14*, 116. [[CrossRef](#)]
181. Sun, F.; Wu, S.; Wang, J.; Guo, S.; Chai, S.; Yang, Z.; Li, L.; Zhang, Y.; Ji, L.; Zhan, S. Effect of glucagon-like peptide-1 receptor agonists on lipid profiles among type 2 diabetes: A systematic review and network meta-analysis. *Clin. Ther.* **2015**, *37*, 225–241.e8. [[CrossRef](#)]
182. Kilkenny, C.; Browne, W.J.; Cuthill, I.C.; Emerson, M.; Altman, D.G. Improving Bioscience Research Reporting: The ARRIVE Guidelines for Reporting Animal Research. *PLoS Biol.* **2010**, *8*, e1000412. [[CrossRef](#)] [[PubMed](#)]
183. Faul, F.; Erdfelder, E.; Lang, A.G.; Buchner, A. G*Power 3: A flexible statistical power analysis program for the social, behavioral, and biomedical sciences. *Behav. Res. Methods* **2007**, *39*, 175–191. [[CrossRef](#)] [[PubMed](#)]
184. Gould, T.D.; Dao, D.T.; Kovacsics, C.E. The open field test. *Neuromethods* **2009**, *42*, 1–20. [[CrossRef](#)]
185. Soares, E.; Prediger, R.D.; Nunes, S.; Castro, A.A.; Viana, S.D.; Lemos, C.; De Souza, C.M.; Agostinho, P.; Cunha, R.A.; Carvalho, E.; et al. Spatial memory impairments in a prediabetic rat model. *Neuroscience* **2013**, *250*, 565–577. [[CrossRef](#)]
186. Akwa, Y.; Ladurelle, N.; Covey, D.F.; Baulieu, E.E. The synthetic enantiomer of pregnenolone sulfate is very active on memory in rats and mice, even more so than its physiological neurosteroid counterpart: Distinct mechanisms? *Proc. Natl. Acad. Sci. USA* **2001**, *98*, 14033–14037. [[CrossRef](#)]
187. Dellu, F.; Fauchey, V.; Moal, M.L.; Simon, H. Extension of a new two-trial memory task in the rat: Influence of environmental context on recognition processes. *Neurobiol. Learn. Mem.* **1997**, *67*, 112–120. [[CrossRef](#)]
188. Dellu, F.; Mayo, W.; Cherkaoui, J.; Le Moal, M.; Simon, H. A two-trial memory task with automated recording: Study in young and aged rats. *Brain Res.* **1992**, *588*, 132–139. [[CrossRef](#)]
189. Morris, R.G.M.; Garrud, P.; Rawlins, J.N.P.; O'Keefe, J. Place navigation impaired in rats with hippocampal lesions. *Nature* **1982**, *297*, 681–683. [[CrossRef](#)]
190. Prediger, R.D.; Batista, L.C.; Medeiros, R.; Pandolfo, P.; Florio, J.C.; Takahashi, R.N. The risk is in the air: Intranasal administration of MPTP to rats reproducing clinical features of Parkinson's disease. *Exp. Neurol.* **2006**, *202*, 391–403. [[CrossRef](#)]
191. García-Nogales, P.; Almeida, A.; Fernández, E.; Medina, J.M.; Bolaños, J.P. Induction of glucose-6-phosphate dehydrogenase by lipopolysaccharide contributes to preventing nitric oxide-mediated glutathione depletion in cultured rat astrocytes. *J. Neurochem.* **1999**, *72*, 1750–1758. [[CrossRef](#)]
192. Fagan, J.M.; Slecicka, B.G.; Sohar, I. Quantitation of oxidative damage to tissue proteins. *Int. J. Biochem. Cell Biol.* **1999**, *31*, 751–757. [[CrossRef](#)]
193. Green, L.C.; Ruiz de Luzuriaga, K.; Wagner, D.A.; Rand, W.; Istfan, N.; Young, V.R.; Tannenbaum, S.R. Nitrate biosynthesis in man. *Proc. Natl. Acad. Sci. USA* **1981**, *78*, 7764–7768. [[CrossRef](#)] [[PubMed](#)]

